# INVERSE RANDOM SOURCE SCATTERING FOR ELASTIC WAVES[*]

### GANG BAO[†], CHUCHU CHEN[‡], AND PEIJUN LI[§]

**Abstract.** This paper is concerned with the direct and inverse random source scattering problems for elastic waves, where the source is assumed to be driven by an additive white noise. Given the source, the direct problem is to determine the displacement of the random wave field. The inverse problem is to reconstruct the mean and variance of the random source from the boundary measurement of the wave field at multiple frequencies. The direct problem is shown to have a unique mild solution by using a constructive proof. Based on the explicit mild solution, Fredholm integral equations of the first kind are deduced for the inverse problem. The regularized block Kaczmarz method is developed to solve the ill-posed integral equations. The convergence is proved for the method. Numerical experiments are shown to demonstrate the effectiveness of the proposed method.

**Key words.** inverse source scattering problem, elastic wave equation, stochastic partial differential equation, Fredholm integral equation

**AMS subject classifications.** 78A46, 65C30

**DOI.** 10.1137/16M1088922

**1. Introduction.** The inverse source scattering problems, an important research subject in inverse scattering theory, are to determine the unknown sources that generate prescribed radiated wave pattens [15, 25]. These problems are largely motivated by applications in medical imaging [21]. A typical example is to use electric or magnetic measurements on the surface of the human body, such as the head, to infer the source currents inside the body, such as the brain, that produce the measured data. Mathematically, the inverse source scattering problems have been widely examined for acoustic and electromagnetic waves by many researchers [1, 2, 4, 5, 10, 11, 17, 19, 32, 33, 36]. For instance, it is known that the inverse source problem does not have a unique solution at a fixed frequency due to the existence of nonradiating sources [18, 23]; it is ill-posed as small variations in the measured data can lead to huge errors in the reconstructions [9].

Although the deterministic counterparts have been well studied, little is known for the stochastic inverse problems due to uncertainties, which are widely introduced to the models for two common reasons: randomness may directly appear in the studied systems [20, 22] and incomplete knowledge of the systems must be modeled by uncertainties [26]. A uniqueness result may be found in [16], where it showed that the auto-correlation function of the random source was uniquely determined every-

[†]School of Mathematical Sciences, Zhejiang University, Hangzhou 310027, China (baog@zju.edu.cn).

[‡]LSEC, ICMSEC, Academy of Mathematics and Systems Science, Chinese Academy of Sciences, Beijing 100190, China (chenchuchu@lsec.cc.ac.cn).

[§]Corresponding author. Department of Mathematics, Purdue University, West Lafayette, IN 47907 (lipeijun@math.purdue.edu).

where outside the source region by the auto-correlation function of the radiated field. Recently, one-dimensional stochastic inverse source problems have been considered in [8, 12, 29], where the governing equations are stochastic ordinary differential equations. Utilizing the Green functions, the authors have presented the first approach in [7] for solving the inverse random source scattering problem in higher dimensions, where the stochastic partial differential equations are considered. An initial effort was made in [31] to study the stability of the inverse random source problem for the one-dimensional Helmholtz equation.

In this paper, we study both the direct and inverse random source scattering problems for elastic waves. Given the source, the direct problem is to determine the displacement of the random wave field. The inverse problem is to reconstruct the mean and variance of the random source from the boundary measurement of the wave field. Recently, the elastic wave scattering problems have received ever increasing attention for their significant applications in many scientific areas such as geophysics and seismology [3, 13, 28, 30]. For example, they have played an important role in the problem for elastic pulse transmission and reflection through the Earth when investigating earthquakes and determining their focus, which is exactly the motivation of this work.

The random source is assumed to be driven by a white noise, which can be thought as the derivative of a Brownian sheet or a multiparameter Brownian motion. The goal is to determine the mean and variance of the random source function by using the same statistics of the displacement of the wave field, which are measured on a boundary enclosing the compactly supported source at multiple frequencies. By constructing a sequence of regular processes approximating the rough white noise, we show that there exists a unique mild solution to the stochastic direct scattering problem. By studying the expectation and variance of the solution, we deduce Fredholm integral equations of the first kind for the inverse problem. It is known that Fredholm integral equations of the first kind are severely ill-posed, which can be clearly seen from the distribution of singular values for our integral equations. It is particularly true for the integral equations of reconstructing the variance. We present well conditioned integral equations via linear combination of the original equations. We propose a regularized block Kaczmarz method to solve the resulting linear system of algebraic equations. Due to the structure of the data, the system is underdetermined and may have infinitely many solutions, among which the minimal norm solution is found. This method is consistent with our multiple frequency data and requires solving a relatively small scale system at each iteration. The convergence of the method is proved under the assumption that the linear system is consistent. Numerical experiments show that the proposed approach is effective to solve the problem.

This work is a nontrivial extension of the method proposed in [7] for the inverse random source scattering problem of the stochastic Helmholtz equation to solve the inverse random source scattering problem of the stochastic Navier equation. Clearly, the elastic wave equation is more challenging due to the coexistence of compressional waves and shear waves that propagate at different speeds. The Green function is more complicated and has higher singularity for the Navier equation than that of the Helmholtz equation does. Hence more sophisticated analysis is required.

The paper is organized as follows. In section 2, we introduce the stochastic Navier equation for elastic waves and discuss the solutions of the deterministic and stochastic direct problems. Section 3 is devoted to the inverse problem, where Fredholm integral equations are deduced and the regularized Kaczmarz method is proposed to reconstruct the mean and the variance. Numerical experiments are presented in section 4

to illustrate the performance of the proposed method. The paper is concluded with general remarks in section 5.

**2. Direct problem.** In this section, we introduce the Navier equation for elastic waves and discuss the solutions of the deterministic and stochastic direct source scattering problems.

**2.1. Problem formulation.** Consider the scattering problem of the two-dimensional stochastic Navier equation in a homogeneous and isotropic medium

$$(2.1) \qquad \mu \Delta \boldsymbol{u} + (\lambda + \mu) \nabla \nabla \cdot \boldsymbol{u} + \omega^2 \boldsymbol{u} = \boldsymbol{f} \quad \text{in } \mathbb{R}^2,$$

where $\omega > 0$ is the angular frequency, $\lambda$ and $\mu$ are the Lamé constants satisfying $\mu > 0$ and $\lambda + \mu > 0$, and $\boldsymbol{u} = (u_1, u_2)^\top$ is the displacement of the random wave field. As a source, the electric current density $\boldsymbol{f} = (f_1, f_2)^\top$ is assumed to be a random function driven by an additive white noise and takes the form

$$(2.2) \qquad \boldsymbol{f}(x) = \boldsymbol{g}(x) + \boldsymbol{h}(x)\dot{W}_x.$$

Here $x = (x_1, x_2)^\top \in \mathbb{R}^2$, $\boldsymbol{g} = (g_1, g_2)^\top$ is a deterministic real vector function, and $\boldsymbol{h} = \text{diag}(h_1, h_2)$ is a deterministic diagonal matrix function with $h_j \geq 0$. We assume that $g_j, h_j, j = 1, 2$ have compact supports contained in the rectangular domain $D \subset \mathbb{R}^2$. $W(x) = (W_1(x), W_2(x))^\top$ is a two-dimensional two-parameter Brownian sheet where $W_1(x)$ and $W_2(x)$ are two independent one-dimensional two-parameter Brownian sheets on the probability space $(\Sigma, \mathcal{F}, P)$. $\dot{W}_x$ is a white noise which can be thought as the derivative of the Brownian sheet $W_x$. To make the paper self-contained, some preliminaries are presented in the appendix for the Brownian sheet, white noise, and corresponding stochastic integrals. In this random source model, $\boldsymbol{g}$ and $\boldsymbol{h}$ can be viewed as the mean and standard deviation of $\boldsymbol{f}$, respectively. Hence $\boldsymbol{h}^2 = \text{diag}(h_1^2, h_2^2)$ is the variance of $\boldsymbol{f}$.

An appropriate radiation condition is needed to complete the formulation of the scattering problem since it is imposed in the open space $\mathbb{R}^2$. Noting $\text{supp}\boldsymbol{f} \subset D$, we have from (2.1) that

$$(2.3) \qquad \mu \Delta \boldsymbol{u} + (\lambda + \mu) \nabla \nabla \cdot \boldsymbol{u} + \omega^2 \boldsymbol{u} = 0 \quad \text{in } \mathbb{R}^2 \setminus \bar{D}.$$

Given a vector function $\boldsymbol{u}$ and a scalar function $u$, define the scalar curl operator and vector curl operator:

$$\text{curl}\boldsymbol{u} = \partial_{x_1} u_2 - \partial_{x_2} u_1, \quad \mathbf{curl}u = (\partial_{x_2} u, -\partial_{x_1} u)^\top.$$

For any solution $\boldsymbol{u}$ of (2.3), we introduce the Helmholtz decomposition

$$(2.4) \qquad \boldsymbol{u} = \nabla \phi + \mathbf{curl}\psi = \boldsymbol{u}_{\text{p}} + \boldsymbol{u}_{\text{s}}.$$

Substituting (2.4) into (2.3), we may verify that $\phi$ and $\psi$ satisfy the Helmholtz equation:

$$(2.5) \qquad \Delta \phi + \kappa_{\text{p}}^2 \phi = 0, \quad \Delta \psi + \kappa_{\text{s}}^2 \psi = 0 \quad \text{in } \mathbb{R}^2 \setminus \bar{D},$$

where $\kappa_{\text{p}}$ and $\kappa_{\text{s}}$ are called the compressional wavenumber and the shear wavenumber, respectively, which are given by

$$\kappa_{\text{p}} = \frac{\omega}{\sqrt{\lambda + 2\mu}}, \quad \kappa_{\text{s}} = \frac{\omega}{\sqrt{\mu}}.$$

Combining (2.4) and (2.5) gives

$$\boldsymbol{u}_{\mathrm{p}} = -\frac{1}{\kappa_{\mathrm{p}}^2}\nabla\nabla\cdot\boldsymbol{u}, \quad \boldsymbol{u}_{\mathrm{s}} = \frac{1}{\kappa_{\mathrm{s}}^2}\mathbf{curl}\mathrm{curl}\boldsymbol{u},$$

which are known as the compressional part and the shear part of the displacement $\boldsymbol{u}$, respectively. The Kupradze–Sommerfeld radiation condition requires that both $\boldsymbol{u}_{\mathrm{p}}$ and $\boldsymbol{u}_{\mathrm{s}}$ satisfy the Sommerfeld radiation condition,

$$(2.6) \qquad \lim_{r\to\infty} r^{1/2}(\partial_r\boldsymbol{u}_{\mathrm{p}} - \mathrm{i}\kappa_{\mathrm{p}}\boldsymbol{u}_{\mathrm{p}}) = 0, \quad \lim_{r\to\infty} r^{1/2}(\partial_r\boldsymbol{u}_{\mathrm{s}} - \mathrm{i}\kappa_{\mathrm{s}}\boldsymbol{u}_{\mathrm{s}}) = 0, \quad r = |x|,$$

uniformly in all directions $\hat{x} = x/|x|$.

Let $B_R = \{x \in \mathbb{R}^2 : |x| < R\}$ be the ball with radius $R$. Denote by $\partial B_R$ the boundary of $B_R$. Let $R$ be large enough such that $\bar{D} \subset B_R$. Given the random electric current density function $\boldsymbol{f}$, i.e., given $\boldsymbol{g}$ and $\boldsymbol{h}$, the direct problem is to determine the random wave field $\boldsymbol{u}$ of the stochastic scattering problem (2.1) and (2.6). The inverse problem is to determine the mean $\boldsymbol{g}$ and the variance $\boldsymbol{h}^2$ of the random source function from the measured random wave field on $\partial B_R$ at a finite number of frequencies $\omega_k, k = 1, \ldots, K$.

**2.2. Deterministic direct problem.** We begin with the solution for the deterministic direct source problem. Let $\boldsymbol{h} = 0$ in (2.2), i.e., no randomness is present in the source. The stochastic scattering problem reduces to the deterministic scattering problem:

$$(2.7) \qquad \begin{cases} \mu\Delta\boldsymbol{u} + (\lambda+\mu)\nabla\nabla\cdot\boldsymbol{u} + \omega^2\boldsymbol{u} = \boldsymbol{g} & \text{in } \mathbb{R}^2, \\ \partial_r\boldsymbol{u}_{\mathrm{p}} - \mathrm{i}\kappa_{\mathrm{p}}\boldsymbol{u}_{\mathrm{p}} = o(r^{-1/2}) & \text{as } r\to\infty, \\ \partial_r\boldsymbol{u}_{\mathrm{s}} - \mathrm{i}\kappa_{\mathrm{s}}\boldsymbol{u}_{\mathrm{s}} = o(r^{-1/2}) & \text{as } r\to\infty. \end{cases}$$

Given $\boldsymbol{g} \in L^2(D)^2$, it is known that the scattering problem (2.7) has a unique solution

$$(2.8) \qquad \boldsymbol{u}(x,\omega) = \int_D \mathbb{G}(x,y,\omega)\boldsymbol{g}(y)\mathrm{d}y,$$

where $\mathbb{G}$ is the Green tensor function of the Navier equation:

$$\mathbb{G}(x,y,\omega) = \frac{\mathrm{i}}{4\mu}H_0^{(1)}(\kappa_{\mathrm{s}}|x-y|)\mathbb{I} + \frac{\mathrm{i}}{4\omega^2}\nabla_x\nabla_x^\top\left[H_0^{(1)}(\kappa_{\mathrm{s}}|x-y|) - H_0^{(1)}(\kappa_{\mathrm{p}}|x-y|)\right].$$

Here $\mathbb{I}$ is the $2 \times 2$ identity matrix, $H_0^{(1)}$ is the Hankel function of the first kind with order zero, and

$$\nabla_x\nabla_x^\top = \begin{pmatrix} \partial_{x_1 x_1} & \partial_{x_1 x_2} \\ \partial_{x_1 x_2} & \partial_{x_2 x_2} \end{pmatrix}.$$

It is known that this Green tensor function has an equivalent form

$$(2.9) \qquad \mathbb{G}(x,y,\omega) = G_1(|x-y|)\mathbb{I} + G_2(|x-y|)\mathbb{J}(x-y),$$

which plays an vital role in derivation of the subsequent regularity analysis. Here for $x \in \mathbb{R}^2\backslash\{0\}$, the matrix $\mathbb{J}$ is given by

$$\mathbb{J}(x) = \frac{xx^\top}{|x|^2}.$$

It is shown in [27] that the functions $G_j$ can be decomposed into

$$(2.10) \qquad G_j(v) = \frac{1}{\pi} \log(v)\Phi_j(v) + \eta_j(v), \quad j = 1, 2,$$

where $\Phi_j$ and $\eta_j$ are analytic functions. Explicitly, we have

$$(2.11) \qquad \Phi_1(v) = \alpha + \beta_1 v^2 + O\left(v^4\right), \quad \Phi_2 = \beta_2 v^2 + O\left(v^4\right)$$

and

$$(2.12) \qquad \eta_1(v) = \gamma_1 + O\left(v^2\right), \quad \eta_2 = \gamma_2 + O\left(v^2\right)$$

for $v \to 0$, where $\alpha$, $\beta_j$, and $\gamma_j$ are constants depending on $\omega$, $\mu$, and $\lambda$.

The following regularity results of the Green tensor function play an important role in the analysis of the stochastic direct scattering problem.

LEMMA 2.1. *Let $\Omega \subset \mathbb{R}^2$ be a bounded domain. Then $\|\mathbb{G}(\cdot, y)\| \in L^2(\Omega)\ \forall y \in \Omega$, where $\|\cdot\|$ is the Frobenius norm.*

*Proof.* Let $a = \sup_{x,y \in \Omega}|x - y|$. We have $\bar{\Omega} \subset B_a(y)$, where $B_a(y)$ is the ball with radius $a$ and center at $y$. Since $\|J(w)\| = 1$, it follows from the expression in (2.9) and (2.10) that we only need to show that

$$\log(|x - y|)|x - y|^m \in L^2(\Omega) \quad \forall\, y \in \Omega,\ m \geq 0.$$

A simple calculation yields

$$\int_\Omega \Big|\log(|x-y|)|x-y|^m\Big|^2 \mathrm{d}x \leq \int_{B_a(y)} \Big|\log(|x-y|)|x-y|^m\Big|^2 \mathrm{d}x$$
$$\lesssim \int_0^a r^{1+2m}\Big|\log(r)\Big|^2 \mathrm{d}r < \infty,$$

which completes the proof. $\qquad\square$

Throughout the paper, $a \lesssim b$ stands for $a \leq Cb$, where $C$ is a positive constant and its specific value is not required but should be clear from the context.

LEMMA 2.2. *Let $\Omega \subset \mathbb{R}^2$ be a bounded domain. We have for $\alpha \in (\frac{3}{2}, \infty)$ that*

$$(2.13) \qquad \int_\Omega \|\mathbb{G}(x, y, \omega) - \mathbb{G}(x, z, \omega)\|^\alpha \mathrm{d}x \lesssim |y - z|^{\frac{3}{2}} \quad \forall\, y, z \in \Omega.$$

*Proof.* It follows from (2.9) and the triangle inequality that

$$\int_\Omega \|\mathbb{G}(x, y, \omega) - \mathbb{G}(x, z, \omega)\|^\alpha \mathrm{d}x$$
$$\lesssim \int_\Omega \Big\|G_1(|x-y|)\mathbb{I} - G_1(|x-z|)\mathbb{I}\Big\|^\alpha \mathrm{d}x$$
$$\quad + \int_\Omega \Big\|G_2(|x-y|)\mathbb{J}(x-y) - G_2(|x-z|)\mathbb{J}(x-z)\Big\|^\alpha \mathrm{d}x$$
$$\lesssim \int_\Omega \Big|G_1(|x-y|) - G_1(|x-z|)\Big|^\alpha \mathrm{d}x + \int_\Omega \Big|G_2(|x-y|) - G_2(|x-z|)\Big|^\alpha \|\mathbb{J}(x-y)\|^\alpha \mathrm{d}x$$
$$\quad + \int_\Omega |G_2(|x-z|)|^\alpha \|\mathbb{J}(x-y) - \mathbb{J}(x-z)\|^\alpha \mathrm{d}x$$
$$=: T_1 + T_2 + T_3.$$

We shall only present the estimates of $T_1$ and $T_3$ since the estimates of $T_1$ and $T_2$ are similar due to $\|\mathbb{J}(x)\| = 1$ and (2.10).

*Step* 1: The estimate of $T_1$. It suffices to estimate the singular part $G_1$ of $T_1$. It follows from (2.10), (2.11), and (2.12) that we have

$$T_1 \lesssim \int_\Omega \Big|\log(|x-y|) - \log(|x-z|)\Big|^\alpha \mathrm{d}x + \int_\Omega \Big||x-y|^p - |x-z|^p\Big|^\alpha \mathrm{d}x$$

$$+ \int_\Omega \Big|\log(|x-y|)|x-y|^p - \log(|x-z|)|x-z|^p\Big|^\alpha \mathrm{d}x$$

$$=: T_1^1 + T_1^2 + T_1^3,$$

where $p = 2$ or $4$.

For the term $T_1^1$, we have

$$T_1^1 = \int_\Omega \Big||x-y| - |x-z|\Big|^{\frac{3}{2}} \Big|\log(|x-y|) - \log(|x-z|)\Big|^{\alpha - \frac{3}{2}}$$

$$\times \left| \int_0^1 \Big(|x-y|t + |x-z|(1-t)\Big)^{-1} \mathrm{d}t \right|^{\frac{3}{2}} \mathrm{d}x$$

$$\leq |y-z|^{\frac{3}{2}} \int_\Omega \Big|\log(|x-y|) - \log(|x-z|)\Big|^{\alpha - \frac{3}{2}} \left| \frac{1}{|x-y|} + \frac{1}{|x-z|} \right|^{\frac{3}{2}} \mathrm{d}x$$

$$\leq |y-z|^{\frac{3}{2}} \left( \int_\Omega \left( \frac{1}{|x-y|} + \frac{1}{|x-z|} \right)^{\frac{9}{5}} \mathrm{d}x \right)^{\frac{5}{6}}$$

$$\times \left( \int_\Omega \Big|\log(|x-y|) - \log(|x-z|)\Big|^{6\alpha - 9} \mathrm{d}x \right)^{\frac{1}{6}},$$

where we have used the Hölder inequality in the last step.

Let $a = \sup_{x,y\in\Omega} |x-y|$ and $b = \sup_{x,z\in\Omega} |x-z|$. We have $\bar{\Omega} \subset B_a(y)$ and $\bar{\Omega} \subset B_b(z)$, where $B_a(y)$ and $B_b(z)$ are the discs with radii $a$ and $b$ and centers at $y$ and $z$, respectively. It is easy to verify that

$$\int_\Omega \left( \frac{1}{|x-y|} + \frac{1}{|x-z|} \right)^{\frac{9}{5}} \mathrm{d}x \lesssim \int_{B_a(y)} \frac{1}{|x-y|^{\frac{9}{5}}} \mathrm{d}x + \int_{B_b(z)} \frac{1}{|x-z|^{\frac{9}{5}}} \mathrm{d}x$$

$$\lesssim \int_0^a r^{-\frac{4}{5}} \mathrm{d}r + \int_0^b r^{-\frac{4}{5}} \mathrm{d}r < \infty$$

and

$$\int_\Omega \Big|\log(|x-y|) - \log(|x-z|)\Big|^{6\alpha-9} \mathrm{d}x$$

$$\lesssim \int_{B_a(y)} \Big|\log(|x-y|)\Big|^{6\alpha-9} \mathrm{d}x + \int_{B_b(z)} \Big|\log(|x-z|)\Big|^{6\alpha-9} \mathrm{d}x$$

$$\lesssim \int_0^a r \Big|\log(r)\Big|^{6\alpha-9} \mathrm{d}r + \int_0^b r \Big|\log(r)\Big|^{6\alpha-9} \mathrm{d}r < \infty.$$

Combining the above estimates gives $T_1^1 \lesssim |y-z|^{\frac{3}{2}}$.

For the term $T_1^2$, using the identity

$$a^p - b^p = (a-b)\big(a^{p-1} + a^{p-2}b + \cdots + ab^{p-2} + b^{p-1}\big),$$

we obtain

$$T_1^2 \lesssim |y - z|^\alpha \int_\Omega \Big[ |x - y|^{(p-1)\alpha} + |x - y|^{(p-2)\alpha}|x - z|^\alpha + \cdots + |x - z|^{(p-1)\alpha} \Big] \mathrm{d}x$$
$$\lesssim |y - z|^\alpha.$$

Applying the technique of estimating the terms $T_1^1$ and $T_1^2$, we get the estimate for the term $T_1^3$:

$$T_1^3 \lesssim \int_\Omega \Big|\log(|x - y|)\Big|^\alpha \Big||x - y|^p - |x - z|^p\Big|^\alpha \mathrm{d}x$$
$$+ \int_\Omega \Big|\log(|x - y|) - \log(|x - z|)\Big|^\alpha |x - z|^{p\alpha} \mathrm{d}x$$
$$\lesssim |y - z|^\alpha \int_\Omega \Big|\log(|x - y|)\Big|^\alpha$$
$$\times \Big[ |x - y|^{(p-1)\alpha} + |x - y|^{(p-2)\alpha}|x - z|^\alpha + \cdots + |x - z|^{(p-1)\alpha} \Big] \mathrm{d}x$$
$$+ |y - z|^{\frac{3}{2}} \int_\Omega \Big|\log(|x - y|) - \log(|x - z|)\Big|^{\alpha - \frac{3}{2}} \left| \frac{1}{|x - y|} + \frac{1}{|x - z|} \right|^{\frac{3}{2}} |x - z|^{p\alpha} \mathrm{d}x$$
$$\lesssim |y - z|^\alpha + |y - z|^{\frac{3}{2}}.$$

Therefore, we obtain $T_1 \leq |y - z|^{\frac{3}{2}}$ for $\alpha > \frac{3}{2}$. Similarly, we may have the estimate $T_2 \leq |y - z|^{\frac{3}{2}}$.

*Step* 2: The estimate of term $T_3$. Recall

$$\mathbb{J}(x) = \begin{bmatrix} J_{11}(x) & J_{12}(x) \\ J_{12}(x) & J_{22}(x) \end{bmatrix} = \begin{bmatrix} \frac{x_1^2}{|x|^2} & \frac{x_1 x_2}{|x|^2} \\ \frac{x_1 x_2}{|x|^2} & \frac{x_2^2}{|x|^2} \end{bmatrix}.$$

A simple calculation yields

$$\|\mathbb{J}(x - y) - \mathbb{J}(x - z)\|^2 = |J_{11}(x - y) - J_{11}(x - z)|^2$$
$$+ 2|J_{12}(x - y) - J_{12}(x - z)|^2 + |J_{22}(x - y) - J_{22}(x - z)|^2.$$

It is easy to verify that

$$|J_{11}(x - y) - J_{11}(x - z)|$$
$$= \left| \frac{(x_1 - y_1)^2}{|x - y|^2} - \frac{(x_1 - z_1)^2}{|x - z|^2} \right| \lesssim \left| \frac{x_1 - y_1}{|x - y|} - \frac{x_1 - z_1}{|x - z|} \right|$$
$$= \left| \frac{(|x - z| - |x - y|)(x_1 - y_1) + |x - y|\big((x_1 - y_1) - (x_1 - z_1)\big)}{|x - y||x - z|} \right|$$
$$\lesssim \frac{|y - z|}{|x - z|}.$$

Similarly, we may show that

$$|J_{22}(x - y) - J_{22}(x - z)| = \left| \frac{(x_2 - y_2)^2}{|x - y|^2} - \frac{(x_2 - z_2)^2}{|x - z|^2} \right| \lesssim \frac{|y - z|}{|x - z|}$$

and

$$|J_{12}(x-y) - J_{12}(x-z)| = \le \frac{|y-z|}{|x-z|} + \frac{|x-y|}{|x-z|^2}|y-z|.$$

Hence

$$\|\mathbb{J}(x-y) - \mathbb{J}(x-z)\| \lesssim \frac{|y-z|}{|x-z|} + \frac{|x-y|}{|x-z|^2}|y-z|,$$

$$\|\mathbb{J}(x-y) - \mathbb{J}(x-z)\| \lesssim \frac{|y-z|}{|x-y|} + \frac{|x-z|}{|x-y|^2}|y-z|.$$

Again, it suffices to consider the singular part $G_2$ of $T_3$. Using (2.10), (2.11), and (2.12), we split the term $T_3$ into two parts:

$$T_3 \lesssim \int_\Omega \left| \log(|x-z|)\left[|x-z|^2 + |x-z|^4\right] + |x-z|^2 \right|^\alpha \|\mathbb{J}(x-y) - \mathbb{J}(x-z)\|^\alpha \mathrm{d}x$$

$$+ \int_\Omega \|\mathbb{J}(x-y) - \mathbb{J}(x-z)\|^\alpha \mathrm{d}x$$

$$=: T_3^1 + T_3^2.$$

For the term $T_3^1$, we have

$$T_3^1 \lesssim |y-z|^\alpha \int_\Omega \left| \log(|x-z|)\left[|x-z|^2 + |x-z|^4\right] + |x-z|^2 \right|^\alpha \left[ \frac{1}{|x-z|^\alpha} + \frac{|x-y|^\alpha}{|x-z|^{2\alpha}} \right] \mathrm{d}x$$

$$\lesssim |y-z|^\alpha.$$

The estimate of $T_3^2$ is more technical. We let $\xi = \frac{y+z}{2}$ and $r = |y-z|$. It is clear to note that

$$T_3^2 = \left( \int_{B_{\frac{r}{4}}(y)} + \int_{B_{\frac{r}{4}}(z)} + \int_{B_{2r}(\xi)\backslash B_{\frac{r}{4}}(y)\cup B_{\frac{r}{4}}(z)} + \int_{\Omega\backslash B_{2r}(\xi)} \right) \|\mathbb{J}(x-y) - \mathbb{J}(x-z)\|^\alpha \mathrm{d}x$$

$$=: I_1 + I_2 + I_3 + I_4.$$

Next we estimate the above four parts. First we have

$$I_1 \lesssim \int_{B_{\frac{r}{4}}(y)} \frac{r^\alpha}{|x-z|^\alpha} + \frac{|x-y|^\alpha}{|x-z|^{2\alpha}} r^\alpha \mathrm{d}x \lesssim \int_{B_{\frac{r}{4}}(y)} \mathrm{d}x \lesssim r^2,$$

where we have utilized the fact that $|x-y| \le \frac{r}{4}$ and $|x-z| > \frac{r}{2}$ for $x \in B_{\frac{r}{4}}(y)$. Similarly, we have

$$I_2 \lesssim \int_{B_{\frac{r}{4}}(z)} \frac{r^\alpha}{|x-y|^\alpha} + \frac{|x-z|^\alpha}{|x-y|^{2\alpha}} r^\alpha \mathrm{d}x \lesssim r^2.$$

For the term $I_3$, we have $|x-z| \ge \frac{r}{4}$ and $\frac{r}{4} \le |x-y| < 3r$ for any $x \in B_{2r}(\xi)\backslash B_{\frac{r}{4}}(y) \cup B_{\frac{r}{4}}(z)$. Thus

$$I_3 \le \int_{B_{2r}(\xi)\backslash B_{\frac{r}{4}}(y)\cup B_{\frac{r}{4}}(z)} \frac{r^\alpha}{|x-z|^\alpha} + \frac{|x-y|^\alpha}{|x-z|^{2\alpha}} r^\alpha \mathrm{d}x \lesssim \int_{B_{2r}(\xi)\backslash B_{\frac{r}{4}}(y)\cup B_{\frac{r}{4}}(z)} \mathrm{d}x \lesssim r^2.$$

It is clear to note for $x \in \Omega \backslash B_{2r}(\xi)$ that

$$\left| \frac{|x - \xi|}{|x - y|} - 1 \right| \leq \frac{|\xi - y|}{|x - y|} \leq \frac{r/2}{2r - r/2} = \frac{1}{3}.$$

We have

$$\frac{2}{3}|x - y| \leq |x - \xi| \leq \frac{4}{3}|x - y|, \quad \frac{2}{3}|x - z| \leq |x - \xi| \leq \frac{4}{3}|x - z|,$$

which give

$$I_4 \lesssim \int_{\Omega \backslash B_{2r}(\xi)} \frac{r^\alpha}{|x - z|^\alpha} + \frac{|x - y|^\alpha}{|x - z|^{2\alpha}} r^\alpha \mathrm{d}x \lesssim \int_{\Omega \backslash B_{2r}(\xi)} \frac{r^\alpha}{|x - \xi|^\alpha} \mathrm{d}x$$

$$\lesssim r^\alpha \int_{2r}^{R} s^{1-\alpha} ds \lesssim r^\alpha \left[ R^{2-\alpha} + (2r)^{2-\alpha} \right] \lesssim r^\alpha + r^2,$$

where $\bar{\Omega} \subset B_R(\xi)$ with $B_R(\xi)$ being the disc with radius $R$ and center at $\xi$. Combining all the estimates in Step 2 gives $T_3 \lesssim |y - z|^{\min\{\alpha, 2\}}$.

The proof is completed by combining Steps 1 and 2. □

**2.3. Stochastic direct problem.** In this section, we discuss the solution for the stochastic direct source scattering problem:

$$(2.14) \quad \begin{cases} \mu \Delta \boldsymbol{u} + (\lambda + \mu)\nabla\nabla \cdot \boldsymbol{u} + \omega^2 \boldsymbol{u} = \boldsymbol{g} + \boldsymbol{h}\dot{W}_x & \text{in } \mathbb{R}^2, \\ \partial_r \boldsymbol{u}_\mathrm{p} - \mathrm{i}\kappa_\mathrm{p} \boldsymbol{u}_\mathrm{p} = o(r^{-1/2}) & \text{as } r \to \infty, \\ \partial_r \boldsymbol{u}_\mathrm{s} - \mathrm{i}\kappa_\mathrm{s} \boldsymbol{u}_\mathrm{s} = o(r^{-1/2}) & \text{as } r \to \infty. \end{cases}$$

Let us first specify the regularity of $\boldsymbol{g}$ and $\boldsymbol{h}$ before discussing the solution of the stochastic scattering problem (2.14). Motivated by the solution of the deterministic direct problem (2.7), we assume that $\boldsymbol{g} \in L^2(D)^2$. The regularity of $\boldsymbol{h}$ is chosen such that the stochastic integral

$$\int_D \mathbb{G}(x, y, \omega)\boldsymbol{h}(y)\mathrm{d}W_y$$

satisfies

$$\mathbf{E}\left( \left| \int_D \mathbb{G}(x, y, \omega)\boldsymbol{h}(y)\mathrm{d}W_y \right|^2 \right) = \int_D \|\mathbb{G}(x, y, \omega)\boldsymbol{h}(y)\|^2 \mathrm{d}y$$

$$\leq \int_D \|\mathbb{G}(x, y, \omega)\|^2 \|\boldsymbol{h}(y)\|^2 \mathrm{d}x < \infty,$$

where Proposition A.2 is used in the above identity.

We only need to consider the singular part of the Green tensor function. It follows from the Hölder inequality that

$$\int_D \left| \log(|x - y|)|x - y|^m \right|^2 \|\boldsymbol{h}(y)\|^2 \mathrm{d}y$$

$$\leq \left( \int_D \left| \log(|x - y|)|x - y|^m \right|^{\frac{2p}{p-2}} \mathrm{d}y \right)^{\frac{p-2}{p}} \left( \int_D \|\boldsymbol{h}(y)\|^p \mathrm{d}y \right)^{\frac{2}{p}}.$$

Since the first term on the right-hand side of the above inequality is a singular integral, $p$ should be chosen such that it is well defined. Let $\rho > 0$ be sufficiently large such that $\bar{D} \subset B_\rho(x)$, where $B_\rho(x)$ is the disc with radius $\rho$ and center at $x$. A simple calculation yields

$$\int_D \left| \log(|x-y|)|x-y|^m \right|^{\frac{2p}{p-2}} \mathrm{d}y \leq \int_{B_\rho(x)} \left| \log(|x-y|)|x-y|^m \right|^{\frac{2p}{p-2}} \mathrm{d}y$$
$$\lesssim \int_0^\rho r^{1+\frac{2mp}{p-2}} \left| \log(r) \right|^{\frac{2p}{p-2}} \mathrm{d}r.$$

It is clear to note that the above integral is well defined when $p > 2$.

From now on, we assume that $h_j \in L^p(D), j = 1, 2$, where $p \in (2, \infty]$. Moreover, we require that $h_j \in C^{0,\eta}(D)$, i.e., $\eta$-Hölder continuous, where $\eta \in (0, 1]$. The Hölder continuity will be used in the analysis for existence of the solution.

The following theorem shows the well-posedness of the solution for the stochastic scattering problem (2.14). The explicit solution will be used to derive Fredholm integral equations for the inverse problem.

THEOREM 2.3. *Let $\Omega \subset \mathbb{R}^2$ be a bounded domain. There exists a unique continuous stochastic process $\boldsymbol{u} : \Omega \to \mathbb{C}$ satisfying*

$$(2.15) \qquad \boldsymbol{u}(x, \omega) = \int_D \mathbb{G}(x, y, \omega) \boldsymbol{g}(y) \mathrm{d}y + \int_D \mathbb{G}(x, y, \omega) \boldsymbol{h}(y) \mathrm{d}W_y, \quad a.s.,$$

*which is called the mild solution of the stochastic scattering problem (2.14).*

*Proof.* First we show that there exists a continuous modification of the random field

$$\boldsymbol{v}(x, \omega) = \int_D \mathbb{G}(x, y, \omega) \boldsymbol{h}(y) \mathrm{d}W_y, \quad x \in \Omega.$$

For any $x, z \in \Omega$, we have from Proposition A.2 and the Hölder inequality that

$$\mathbf{E}(|\boldsymbol{v}(x,\omega) - \boldsymbol{v}(z,\omega)|^2) = \int_D \left\| \Big( \mathbb{G}(x, y, \omega) - \mathbb{G}(z, y, \omega) \Big) \boldsymbol{h}(y) \right\|^2 \mathrm{d}y$$
$$\leq \left( \int_D \|\mathbb{G}(x, y, \omega) - \mathbb{G}(z, y, \omega)\|^{\frac{2p}{p-2}} \mathrm{d}y \right)^{\frac{p-2}{p}} \left( \int_D \|\boldsymbol{h}(y)\|^p \mathrm{d}y \right)^{\frac{2}{p}}.$$

For $p > 2$, it follows from (2.13) that

$$\int_D \|\mathbb{G}(x, y, \omega) - \mathbb{G}(z, y, \omega)\|^{\frac{2p}{p-2}} \mathrm{d}y \lesssim |x - z|^{\frac{3}{2}},$$

which gives

$$\mathbf{E}(|\boldsymbol{v}(x,\omega) - \boldsymbol{v}(z,\omega)|^2) \lesssim \|\boldsymbol{h}\|^2_{L^p(D)^2} |x - z|^{\frac{3p-6}{2p}}.$$

Since $\boldsymbol{v}(x,\kappa) - \boldsymbol{v}(z,\kappa)$ is a random Gaussian variable, we have (cf. [24, Proposition 3.14]) for any integer $q$ that

$$\mathbf{E}(|\boldsymbol{v}(x,\omega) - \boldsymbol{v}(z,\omega)|^{2q}) \lesssim \left( \mathbf{E}(|\boldsymbol{v}(x,\omega) - \boldsymbol{v}(z,\omega)|^2) \right)^q \lesssim \|\boldsymbol{h}\|^{2q}_{L^p(D)^2} |x - z|^{\frac{q(3p-6)}{2p}}.$$

Taking $q > \frac{2p}{3p-6}$, we obtain from Kolmogorov's continuity theorem that there exists a P-a.s. continuous modification of the random field $\boldsymbol{v}$.

Clearly, the uniqueness of the mild solution comes from the solution representation formula (2.15), which depends only on the Green function $\mathbb{G}$ and the source functions $\boldsymbol{g}$ and $\boldsymbol{h}$.

Next we present a constructive proof to show the existence. We construct a sequence of processes $\dot{W}_x^n$ satisfying $\boldsymbol{h}\dot{W}^n \in L^2(D)^2$ and a sequence

$$\boldsymbol{v}^n(x,\omega) = \int_D \mathbb{G}(x,y,\omega)\boldsymbol{h}(y)\mathrm{d}W_y^n, \quad x \in \Omega,$$

which satisfies $\boldsymbol{v}^n \to \boldsymbol{v}$ in $L^2(\Omega)$ a.s. as $n \to \infty$.

Let $\mathcal{T}_n = \cup_{j=1}^n K_j$ be a regular triangulation of $D$, where $K_j$ are triangles. Denote

$$\xi_j = |K_j|^{-\frac{1}{2}} \int_{K_j} \mathrm{d}W_x, \quad 1 \le j \le n,$$

where $|K_j|$ is the area of the $K_j$. It is known in [14] that $\xi_j$ is a family of independent identically distributed normal random variables with mean zero and variance one. The piecewise constant approximation sequence is given by

$$\dot{W}_x^n = \sum_{j=1}^n |K_j|^{-\frac{1}{2}} \xi_j \chi_j(x),$$

where $\chi_j$ is the characteristic function of $K_j$. Clearly we have for any $p \ge 1$ that

$$\mathbf{E}\big(\|\dot{W}^n\|_{L^p(D)^2}^p\big) = \mathbf{E}\Big(\int_D \Big|\sum_{j=1}^n |K_j|^{-\frac{1}{2}} \xi_j \chi_j(x)\Big|^p \mathrm{d}x\Big) \lesssim \mathbf{E}\Big(\int_D \sum_{j=1}^n |K_j|^{-\frac{p}{2}} |\xi_j|^p \chi_j(x)\mathrm{d}x\Big)$$

$$= \sum_{j=1}^n \mathbf{E}(|\xi_j|^p)|K_j|^{1-\frac{p}{2}} < \infty,$$

which shows that $\dot{W}^n \in L^p(D)^2, p \ge 1$. It follows from the Hölder inequality that $\boldsymbol{h}\dot{W}^n \in L^2(D)^2$.

Using Proposition A.2, we have that

$$\mathbf{E}\left(\int_\Omega \left|\int_D \mathbb{G}(x,y,\omega)\boldsymbol{h}(y)\mathrm{d}W_y - \int_D \mathbb{G}(x,y,\omega)\boldsymbol{h}(y)\mathrm{d}W_y^n\right|^2 \mathrm{d}x\right)$$

$$= \mathbf{E}\left(\int_\Omega \left|\sum_{j=1}^n \int_{K_j} \mathbb{G}(x,y,\omega)\boldsymbol{h}(y)\mathrm{d}W_y - \sum_{j=1}^n |K_j|^{-1} \int_{K_j} \mathbb{G}(x,z,\omega)\boldsymbol{h}(z)\mathrm{d}z \int_{K_j} \mathrm{d}W_y\right|^2 \mathrm{d}x\right)$$

$$= \mathbf{E}\left(\int_\Omega \left|\sum_{j=1}^n \int_{K_j} \int_{K_j} |K_j|^{-1} (\mathbb{G}(x,y,\omega)\boldsymbol{h}(y) - \mathbb{G}(x,z,\omega)\boldsymbol{h}(z))\mathrm{d}z\mathrm{d}W_y\right|^2 \mathrm{d}x\right)$$

$$= \int_\Omega \left(\sum_{j=1}^n \int_{K_j} \left||K_j|^{-1} \int_{K_j} (\mathbb{G}(x,y,\omega)\boldsymbol{h}(y) - \mathbb{G}(x,z,\omega)\boldsymbol{h}(z))\mathrm{d}z\right|^2 \mathrm{d}y\right) \mathrm{d}x$$

$$\le \int_\Omega \left(\sum_{j=1}^n |K_j|^{-1} \int_{K_j} \int_{K_j} \|\mathbb{G}(x,y,\omega)\boldsymbol{h}(y) - \mathbb{G}(x,z,\omega)\boldsymbol{h}(z)\|^2 \mathrm{d}z\mathrm{d}y\right) \mathrm{d}x$$

$$= \sum_{j=1}^n |K_j|^{-1} \int_{K_j} \int_{K_j} \int_\Omega \|\mathbb{G}(x,y,\omega)\boldsymbol{h}(y) - \mathbb{G}(x,z,\omega)\boldsymbol{h}(z)\|^2 \mathrm{d}x\mathrm{d}z\mathrm{d}y.$$

Using the triangle and Cauchy–Schwarz inequalities, we get

$$\int_\Omega \|\mathbb{G}(x,y,\omega)\boldsymbol{h}(y) - \mathbb{G}(x,z,\omega)\boldsymbol{h}(z)\|^2 \mathrm{d}x \lesssim \int_\Omega \|\mathbb{G}(x,y,\omega) - \mathbb{G}(x,z,\omega)\|^2 \|\boldsymbol{h}(y)\|^2 \mathrm{d}x$$
$$+ \int_\Omega \|\mathbb{G}(x,z,\omega)\|^2 \|\boldsymbol{h}(y) - \boldsymbol{h}(z)\|^2 \mathrm{d}x.$$

It follows from (2.13), Lemma 2.1, and the $\eta$-Hölder continuity of $\boldsymbol{h}$ that

$$\int_\Omega \|\mathbb{G}(x,y,\omega)\boldsymbol{h}(y) - \mathbb{G}(x,z,\omega)\boldsymbol{h}(z)\|^2 \mathrm{d}x \lesssim \|\boldsymbol{h}(y)\|^2 |y-z|^{\frac{3}{2}} + |y-z|^{2\eta},$$

which gives

$$\mathbf{E}\left(\int_\Omega \left|\int_D \mathbb{G}(x,y,\omega)\boldsymbol{h}(y)\mathrm{d}W_y - \int_D \mathbb{G}(x,y,\omega)\boldsymbol{h}(y)\mathrm{d}W_y^n\right|^2 \mathrm{d}x\right)$$
$$\lesssim \sum_{j=1}^n |K_j|^{-1} \int_{K_j}\int_{K_j} \|\boldsymbol{h}(z)\|^2 |y-z|^{\frac{3}{2}} \mathrm{d}z\mathrm{d}y + \sum_{j=1}^n |K_j|^{-1} \int_{K_j}\int_{K_j} |y-z|^{2\eta} \mathrm{d}z\mathrm{d}y$$
$$\leq \|\boldsymbol{h}\|_{L^2(D)^2}^2 \max_{1\leq j\leq n}(\mathrm{diam}K_j)^{\frac{3}{2}} + |D| \max_{1\leq j\leq n}(\mathrm{diam}K_j)^{2\eta} \to 0$$

as $n \to \infty$ since the diameter of $K_j \to 0$ as $n \to \infty$.

For each $n \in \mathbb{N}$, we consider the scattering problem:

$$(2.16) \qquad \begin{cases} \mu\Delta\boldsymbol{u}^n + (\lambda+\mu)\nabla\nabla\cdot\boldsymbol{u}^n + \omega^2\boldsymbol{u}^n = \boldsymbol{g} + \boldsymbol{h}\dot{W}_x^n & \text{in } \mathbb{R}^2, \\ \partial_r\boldsymbol{u}_{\mathrm{p}}^n - \mathrm{i}\kappa_{\mathrm{p}}\boldsymbol{u}_{\mathrm{p}}^n = o(r^{-1/2}) & \text{as } r \to \infty, \\ \partial_r\boldsymbol{u}_{\mathrm{s}}^n - \mathrm{i}\kappa_{\mathrm{s}}\boldsymbol{u}_{\mathrm{s}}^n = o(r^{-1/2}) & \text{as } r \to \infty. \end{cases}$$

It follows from $\boldsymbol{h}\dot{W}_x^n \in L^2(D)^2$ that the problem (2.16) has a unique solution which is given by

$$(2.17) \qquad \boldsymbol{u}^n(x,\omega) = \int_D \mathbb{G}(x,y,\omega)\boldsymbol{g}(y)\mathrm{d}y + \int_D \mathbb{G}(x,y,\omega)\boldsymbol{h}(y)\mathrm{d}W_y^n.$$

Since $\mathbf{E}(\|\boldsymbol{v}^n - \boldsymbol{v}\|_{L^2(\Omega)^2}^2) \to 0$ as $n \to \infty$, there exists a subsequence still denoted as $\{\boldsymbol{v}^n\}$ which converges to $\boldsymbol{v}$ a.s.. Letting $n \to \infty$ in (2.17), we obtain the mild solution (2.15) and complete the proof. $\qquad\square$

It is clear to note that the mild solution of the stochastic direct problem (2.15) reduces to the solution of the deterministic direct problem (2.8) when $\boldsymbol{h} = 0$, i.e., no randomness is present in the source.

**3. Stochastic inverse problem.** In this section, we derive the Fredholm integral equations and present a regularized Kaczmarz method to solve the stochastic inverse problem by using multiple frequency data.

**3.1. Integral equations.** Recall the mild solution of the stochastic direct scattering problem at angular frequency $\omega_k$:

$$(3.1) \qquad \boldsymbol{u}(x,\omega_k) = \int_D \mathbb{G}(x,y,\omega_k)\boldsymbol{g}(y)\mathrm{d}y + \int_D \mathbb{G}(x,y,\omega_k)\boldsymbol{h}(y)\mathrm{d}W_y.$$

Taking the expectation on both sides of (3.1) and using Proposition A.3, we obtain

$$\mathbf{E}(\boldsymbol{u}(x,\omega_k)) = \int_D \mathbb{G}(x,y,\omega_k)\boldsymbol{g}(y)\mathrm{d}y,$$

which is a complex-valued Fredholm integral equation of the first kind and may be used to reconstruct $\boldsymbol{g}$. However, it is more convenient to solve real-valued equations. We shall split all the complex-valued quantities into their real and imaginary parts, which also allows us to deduce the equations for the variance.

Let $\boldsymbol{u} = \mathrm{Re}\boldsymbol{u} + \mathrm{i}\mathrm{Im}\boldsymbol{u}$ and $\mathbb{G} = \mathrm{Re}\mathbb{G} + \mathrm{i}\mathrm{Im}\mathbb{G}$, where

$$\mathrm{Re}\mathbb{G}(x,y,\omega_k) = \begin{bmatrix} G_{\mathrm{Re}}^{[11]}(x,y,\omega_k) & G_{\mathrm{Re}}^{[12]}(x,y,\omega_k) \\ G_{\mathrm{Re}}^{[21]}(x,y,\omega_k) & G_{\mathrm{Re}}^{[22]}(x,y,\omega_k) \end{bmatrix},$$

$$\mathrm{Im}\mathbb{G}(x,y,\omega_k) = \begin{bmatrix} G_{\mathrm{Im}}^{[11]}(x,y,\omega_k) & G_{\mathrm{Im}}^{[12]}(x,y,\omega_k) \\ G_{\mathrm{Im}}^{[21]}(x,y,\omega_k) & G_{\mathrm{Im}}^{[22]}(x,y,\omega_k) \end{bmatrix}.$$

The entries $G_{\mathrm{Re}}^{[ij]}$ and $G_{\mathrm{Im}}^{[ij]}$ are given in Appendix B.

The mild solution (3.1) can be split into the real and imaginary parts:

$$\begin{aligned} (3.2) \quad & \mathrm{Re}\boldsymbol{u}(x,\omega_k) = \int_D \mathrm{Re}\mathbb{G}(x,y,\omega_k)\boldsymbol{g}(y)\mathrm{d}y + \int_D \mathrm{Re}\mathbb{G}(x,y,\omega_k)\boldsymbol{h}(y)\mathrm{d}W_y, \\ & \mathrm{Im}\boldsymbol{u}(x,\omega_k) = \int_D \mathrm{Im}\mathbb{G}(x,y,\omega_k)\boldsymbol{g}(y)\mathrm{d}y + \int_D \mathrm{Im}\mathbb{G}(x,y,\omega_k)\boldsymbol{h}(y)\mathrm{d}W_y. \end{aligned}$$

Using Proposition A.3 again, we take the expectation on both sides of (3.2) and obtain real-valued Fredholm integral equations of the first kind to reconstruct $\boldsymbol{g}$:

$$\mathbf{E}(\mathrm{Re}\boldsymbol{u}(x,\omega_k)) = \int_D \mathrm{Re}\mathbb{G}(x,y,\omega_k)\boldsymbol{g}(y)\mathrm{d}y,$$

$$\mathbf{E}(\mathrm{Im}\boldsymbol{u}(x,\omega_k)) = \int_D \mathrm{Im}\mathbb{G}(x,y,\omega_k)\boldsymbol{g}(y)\mathrm{d}y,$$

which are equivalent to the following equations in componentwise forms:

$$(3.3) \qquad \mathbf{E}(\mathrm{Re}u_1(x,\omega_k)) = \int_D \left[ G_{\mathrm{Re}}^{[11]}(x,y,\omega_k)g_1(y) + G_{\mathrm{Re}}^{[12]}(x,y,\omega_k)g_2(y) \right]\mathrm{d}y,$$

$$(3.4) \qquad \mathbf{E}(\mathrm{Re}u_2(x,\omega_k)) = \int_D \left[ G_{\mathrm{Re}}^{[21]}(x,y,\omega_k)g_1(y) + G_{\mathrm{Re}}^{[22]}(x,y,\omega_k)g_2(y) \right]\mathrm{d}y,$$

$$(3.5) \qquad \mathbf{E}(\mathrm{Im}u_1(x,\omega_k)) = \int_D \left[ G_{\mathrm{Im}}^{[11]}(x,y,\omega_k)g_1(y) + G_{\mathrm{Im}}^{[12]}(x,y,\omega_k)g_2(y) \right]\mathrm{d}y,$$

$$(3.6) \qquad \mathbf{E}(\mathrm{Im}u_2(x,\omega_k)) = \int_D \left[ G_{\mathrm{Im}}^{[21]}(x,y,\omega_k)g_1(y) + G_{\mathrm{Im}}^{[22]}(x,y,\omega_k)g_2(y) \right]\mathrm{d}y.$$

We notice from the above equations, (3.3)–(3.6), that the reconstruction of $\boldsymbol{g}$ looks like the one for the deterministic inverse problem except that the known boundary data is given by the expectation of the radiation wave field on the surface $\partial B_R$. It is known that Fredholm integral equations of the first kind are ill-posed due to the rapidly decaying singular values of matrices from the discretized integral kernels. Appropriate regularization methods are needed to recover the information about the solutions as stably as possible. As a representative example, Figure 1 plots the singular
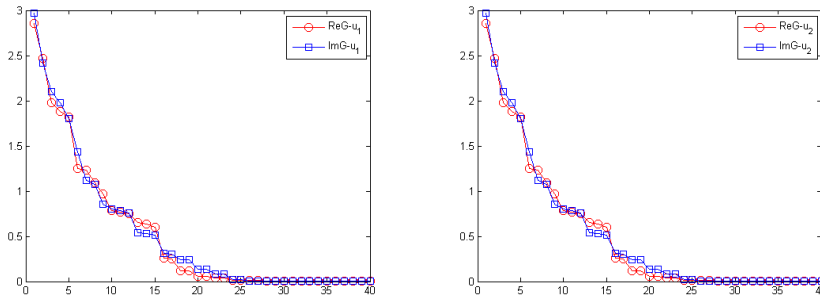
FIG. 1. *Singular values of the Fredholm integral equations for the reconstruction of $\boldsymbol{g}$: (left) component for $u_1$; (right) component for $u_2$.*

values of the matrices for the Fredholm integral equations (3.3)–(3.6) at $\omega = 1.9\pi$. We can observe similar decaying patterns for the singular values of (3.3) and (3.5) for the component $u_1$ and of (3.4) and (3.6) for the component $u_2$.

To reconstruct the variance $\boldsymbol{h}^2$, we use Proposition A.3 to obtain

$$
\mathbf{E}\left(\left|\int_D \mathrm{Re}\mathbb{G}(x,y,\omega_k)\boldsymbol{h}(y)\mathrm{d}W_y\right|^2\right)
$$
$$
= \int_D \|\mathrm{Re}\mathbb{G}(x,y,\omega_k)\boldsymbol{h}(y)\|^2 \mathrm{d}y
$$
$$
= \int_D \left[(G_{\mathrm{Re}}^{[11]}(x,y,\omega_k))^2 + (G_{\mathrm{Re}}^{[21]}(x,y,\omega_k))^2\right]h_1^2(y)\mathrm{d}y
$$
$$
+ \int_D \left[(G_{\mathrm{Re}}^{[12]}(x,y,\omega_k))^2 + (G_{\mathrm{Re}}^{[22]}(x,y,\omega_k))^2\right]h_2^2(y)\mathrm{d}y
$$

and

$$
\mathbf{E}\left(\left|\int_D \mathrm{Im}\mathbb{G}(x,y,\omega_k)\boldsymbol{h}(y)\mathrm{d}W_y\right|^2\right)
$$
$$
= \int_D \|\mathrm{Im}\mathbb{G}(x,y,\omega_k)\boldsymbol{h}(y)\|^2 \mathrm{d}y
$$
$$
= \int_D \left[(G_{\mathrm{Im}}^{[11]}(x,y,\omega_k))^2 + (G_{\mathrm{Im}}^{[21]}(x,y,\omega_k))^2\right]h_1^2(y)\mathrm{d}y
$$
$$
+ \int_D \left[(G_{\mathrm{Im}}^{[12]}(x,y,\omega_k))^2 + (G_{\mathrm{Im}}^{[22]}(x,y,\omega_k))^2\right]h_2^2(y)\mathrm{d}y.
$$

Taking the variance on both sides of (3.2), we get

$$
\mathbf{V}(\mathrm{Re}\boldsymbol{u}(x,\omega_k)) = \int_D \left[(G_{\mathrm{Re}}^{[11]}(x,y,\omega_k))^2 + (G_{\mathrm{Re}}^{[21]}(x,y,\omega_k))^2\right]h_1^2(y)\mathrm{d}y
$$
$$
+ \int_D \left[(G_{\mathrm{Re}}^{[12]}(x,y,\omega_k))^2 + (G_{\mathrm{Re}}^{[22]}(x,y,\omega_k))^2\right]h_2^2(y)\mathrm{d}y,
$$
$$
\mathbf{V}(\mathrm{Im}\boldsymbol{u}(x,\omega_k)) = \int_D \left[(G_{\mathrm{Im}}^{[11]}(x,y,\omega_k))^2 + (G_{\mathrm{Im}}^{[21]}(x,y,\omega_k))^2\right]h_1^2(y)\mathrm{d}y
$$
$$
+ \int_D \left[(G_{\mathrm{Im}}^{[12]}(x,y,\omega_k))^2 + (G_{\mathrm{Im}}^{[22]}(x,y,\omega_k))^2\right]h_2^2(y)\mathrm{d}y,
$$

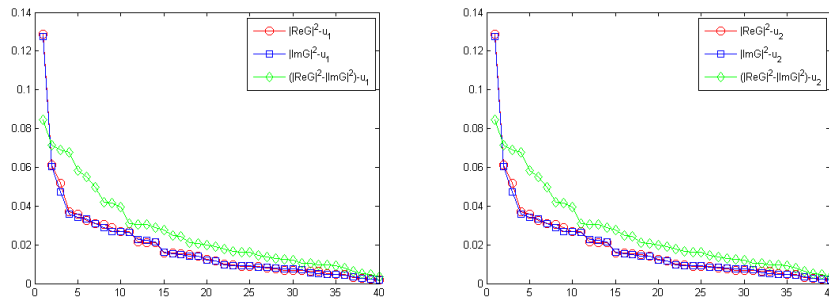which are the Fredholm integral equations of the first kind to reconstruct the variance.

FIG. 2. *Singular values of the Fredholm integral equations for the reconstruction of $\boldsymbol{h}^2$: (left) component of $u_1$; (right) component of $u_2$.*

Again, we consider the variance of components $u_1$ and $u_2$:

$$(3.7) \quad \mathbf{V}(\mathrm{Re}u_1(x,\omega_k)) = \int_D \left[ \left(G_{\mathrm{Re}}^{[11]}(x,y,\omega_k)\right)^2 h_1^2(y) + \left(G_{\mathrm{Re}}^{[12]}(x,y,\omega_k)\right)^2 h_2^2(y) \right] \mathrm{d}y,$$

$$(3.8) \quad \mathbf{V}(\mathrm{Re}u_2(x,\omega_k)) = \int_D \left[ \left(G_{\mathrm{Re}}^{[21]}(x,y,\omega_k)\right)^2 h_1^2(y) + \left(G_{\mathrm{Re}}^{[22]}(x,y,\omega_k)\right)^2 h_2^2(y) \right] \mathrm{d}y,$$

$$(3.9) \quad \mathbf{V}(\mathrm{Im}u_1(x,\omega_k)) = \int_D \left[ \left(G_{\mathrm{Im}}^{[11]}(x,y,\omega_k)\right)^2 h_1^2(y) + \left(G_{\mathrm{Im}}^{[12]}(x,y,\omega_k)\right)^2 h_2^2(y) \right] \mathrm{d}y,$$

$$(3.10) \quad \mathbf{V}(\mathrm{Im}u_2(x,\omega_k)) = \int_D \left[ \left(G_{\mathrm{Im}}^{[21]}(x,y,\omega_k)\right)^2 h_1^2(y) + \left(G_{\mathrm{Im}}^{[22]}(x,y,\omega_k)\right)^2 h_2^2(y) \right] \mathrm{d}y.$$

To investigate ill-posedness of the above four equations, we plot their singular values in Figure 2. It can be seen that (3.7), (3.9) and (3.8), (3.10) show almost identical distributions of the singular values for components $u_1$ and $u_2$, respectively. The singular values decay exponentially to zeros, and there is a big gap between the few leading singular values and the rests. Hence it is severely ill-posed to use directly either (3.7) or (3.9) and (3.8) or (3.10) to reconstruct $h_1^2$ and $h_2^2$. Subtracting (3.9) from (3.7) and (3.10) from (3.8), we obtain the improved equations to reconstruct $h_1^2$ and $h_2^2$:

$$(3.11) \quad \mathbf{V}(\mathrm{Re}u_1(x,\omega_k)) - \mathbf{V}(\mathrm{Im}u_1(x,\omega_k))$$
$$= \int_D \left[ \left(G_{\mathrm{Re}}^{[11]}(x,y,\omega_k)\right)^2 - \left(G_{\mathrm{Im}}^{[11]}(x,y,\omega_k)\right)^2 \right] h_1^2(y)\mathrm{d}y$$
$$+ \int_D \left[ \left(G_{\mathrm{Re}}^{[12]}(x,y,\omega_k)\right)^2 - \left(G_{\mathrm{Im}}^{[12]}(x,y,\omega_k)\right)^2 \right] h_2^2(y)\mathrm{d}y,$$

$$(3.12) \quad \mathbf{V}(\mathrm{Re}u_2(x,\omega_k)) - \mathbf{V}(\mathrm{Im}u_2(x,\omega_k))$$
$$= \int_D \left[ \left(G_{\mathrm{Re}}^{[21]}(x,y,\omega_k)\right)^2 - \left(G_{\mathrm{Im}}^{[21]}(x,y,\omega_k)\right)^2 \right] h_1^2(y)\mathrm{d}y$$
$$+ \int_D \left[ \left(G_{\mathrm{Re}}^{[22]}(x,y,\omega_k)\right)^2 - \left(G_{\mathrm{Im}}^{[22]}(x,y,\omega_k)\right)^2 \right] h_2^2(y)\mathrm{d}y.$$

In fact, it is clear to note in Figure 2 that the singular values of (3.11) and (3.12) display better behavior that those of (3.7), (3.9) and (3.8), (3.10). They decay more slowly and distribute more uniformly. Numerically, (3.11) and (3.12) do give much better reconstructions. We will only show the results for (3.11) and (3.12) in the numerical experiments.

**3.2. Numerical method.** In this section, we present a regularized block Kacz-marz method to solve the ill-posed integral equations (3.3)–(3.6) and (3.11)–(3.12). First, these integrals need to be discretized. Since the numerical integration are almost the same for these integrals, we use the integral equation (3.3) as an example to illustrate the detailed discretization steps in the following.

Recall that $D$ is a rectangular domain and $B_R$ is a ball with radius $R$, where $R$ is large enough such that $\bar{D} \subset B_R$. Define $D = \{(y_1, y_2)^\top \in \mathbb{R}^2 : a \leq y_1 \leq b, c \leq y_2 \leq d\}$. Let the interval $[a, b]$ be subdivided into $n_1$ subintervals of equal width $\Delta_1 = (b - a)/n_1$ by using the equally spaced sample points $y_{1,\ell_1} = a + \ell_1 \Delta_1, \ell_1 = 0, \ldots, n_1$. Similarly, let the interval $[c, d]$ be subdivided into $n_2$ subintervals of equal width $\Delta_2 = (d - c)/n_2$ by using the equally spaced sample points $y_{2,\ell_2} = c + \ell_2 \Delta_2, \ell_2 = 0, \ldots, n_2$. Define $\ell = (\ell_1, \ell_2)$ and $y_\ell = (y_{1,\ell_1}, y_{2,\ell_2})^\top \in \mathbb{R}^2$. The boundary $\partial B_R$ is also divided into a uniform grid $x_i = (R \cos \theta_i, R \sin \theta_i)^\top \in \mathbb{R}^2, \theta_i = (i - 1)2\pi/m, i = 1, \ldots, m$. Since $x_i \in \partial B_R$ and $y_\ell \in D$, we have $x_i \neq y_\ell$ for $i = 1, \ldots, m, \ell_1 = 0, \ldots, n_1, \ell_2 = 0, \ldots, n_2$. Thus the Green functions in (3.3) have no singularity and are smooth. Noting that $g_1, g_2$ have compact supports contained in $D$, we obtain from (3.3) by using the composite trapezoidal rule that

$$\sum_{\ell_1=1}^{n_1-1} \sum_{\ell_2=1}^{n_2-1} \Delta_1 \Delta_2 \left( G_{\mathrm{Re}}^{[11]}(x_i, y_\ell, \omega_k) g_1(y_\ell) + G_{\mathrm{Re}}^{[12]}(x_i, y_\ell, \omega_k) g_2(y_\ell) \right)$$
$$+ \mathcal{O}(\Delta_1^2 + \Delta_2^2) = \mathbf{E}(\mathrm{Re} u_1(x_i, \omega_k)), \quad i = 1, \ldots, m.$$

Let $n = 2(n_1 - 1)(n_2 - 1)$. Dropping the discretization error, we may formally consider the matrix equations:

$$(3.13) \qquad\qquad\qquad A_k q = p_k, \quad k = 1, \ldots, K,$$

where $A_k : \mathbb{R}^n \to \mathbb{R}^m$ is an $m \times n$ matrix given by

$$A_k = \Delta_1 \Delta_2 \left[ \cdots G_{\mathrm{Re}}^{[11]}(x_i, y_\ell, \omega_k) \cdots \Big| \cdots G_{\mathrm{Re}}^{[12]}(x_i, y_\ell, \omega_k) \cdots \right],$$
$$q = \left( \cdots g_1(y_\ell) \cdots \big| \cdots g_2(y_\ell) \cdots \right)^\top \in \mathbb{R}^n,$$
$$p_k = \left( \mathbf{E}(\mathrm{Re} u_1(x_1, \omega_k)), \ldots, \mathbf{E}(\mathrm{Re} u_1(x_m, \omega_k)) \right)^\top \in \mathbb{R}^m$$

for $i = 1, \ldots, m, \ell = (\ell_1, \ell_2), \ell_1 = 1, \ldots, n_1 - 1, \ell_2 = 1, \ldots, n_2 - 1$.

*Remark* 3.1. In practice, the number of rows of $A_k$, which is the number of data points, is usuall small. For example, we take 20 data points on $\partial B_R$, i.e., $m = 20$, in our numerical experiments. The rectangular domain $D$ is uniformly divided into $20 \times 20$ small rectangles, i.e., $n_1 = n_2 = 20$ and $n = 2 \times 19 \times 19 = 722$. So the linear system (3.13) is an underdetermined system with $m \ll n$. Since $A_k$ has as few as 20 rows, it is unlikely that these rows are linearly dependent. Therefore, we assume that $A_k$ has linearly independent rows.

*Remark* 3.2. For other integral equations, $A_k$ is the matrix arising from discretizing the integral kernels, $q$ represents the unknown $g_1, g_2$ or $h_1^2, h_2^2$, and $p_k$ is the given data. The resulting linear system (3.13) is underdetermined since the number of measurements is less than the number of unknowns.

Equivalently, the system (3.13) can be written as

$$(3.14) \qquad\qquad\qquad\qquad Aq = p,$$

where

$$A = \begin{bmatrix} A_1 \\ \vdots \\ A_K \end{bmatrix}, \quad p = \begin{bmatrix} p_1 \\ \vdots \\ p_K \end{bmatrix}.$$

*Remark* 3.3. In practice, the total number of frequencies $K$ cannot be too large either, e.g., $K = 20$, so that $mK < n$. Therefore, the system (3.14) is still underdetermined and may have infinitely many solutions. We are seeking the minimal norm solution, which is briefly introduced in Appendix C.

Next we consider the block Kaczmarz method, which is an iterative method for solving linear system of equations [34]. Given an initial guess $q^0$, the classical Kaczmarz method for solving (3.13) reads as follows: For $l = 0, 1, \ldots,$

$$(3.15) \qquad \begin{cases} q_0 = q^l, \\ q_k = q_{k-1} + A_k^\top (A_k A_k^\top)^{-1}(p_k - A_k q_{k-1}), \quad k = 1, \ldots, K, \\ q^{l+1} = q_K. \end{cases}$$

There are two loops in the algorithm: the outer loop is carried for the iterative index $l$ and the inner loop is taken for the frequency $\omega_k$. We state the convergence theorem of the classical Kaczmarz method. The proof can be found in [34, Theorem 3.6].

THEOREM 3.4. *Assume that the system* (3.13) *is consistent and has a solution. If the initial guess* $q^0 \in \mathcal{R}(A^\top)$, *e.g.,* $q^0 = 0$, *then* $q^l$ *converges, as* $l \to \infty$, *to the minimal norm solution* $q^\dagger$ *of* (3.13).

In (3.15), $A_k$ is assumed to have linearly independent rows and thus has a full rank, and the matrix $A_k A_k^\top$ is invertible, but it is ill-conditioned due to the ill-posedness of the problem. A regularization technique is needed to make the method stable. We propose a regularized block Kaczmarz method: Given an initial guess $q_\gamma^0$, for $l = 0, 1, \ldots,$

$$(3.16) \qquad \begin{cases} q_0 = q_\gamma^l, \\ q_k = q_{k-1} + A_k^\top (\gamma I + A_k A_k^\top)^{-1}(p_k - A_k q_{k-1}), \quad k = 1, \ldots, K, \\ q_\gamma^{l+1} = q_K, \end{cases}$$

where the regularization parameter $\gamma$ is a small positive number and $I$ is the identity matrix. The rest of this section is to analyze the convergence of (3.16).

Letting $u_j = (\gamma I + A_j A_j^\top)^{-1}(p_j - A_j q_{j-1})$, we have from (3.16) that

$$q_k = q_0 + \sum_{j=1}^{k} A_j^\top u_j$$

$$= q_0 + \sum_{j=1}^{k-1} A_j^\top u_j + A_k^\top \left(\gamma I + A_k A_k^\top\right)^{-1} \left(p_k - A_k q_0 - \sum_{j=1}^{k-1} A_k A_j^\top u_j\right).$$

Due to the injectivity of $A_k^\top$, we obtain

$$(3.17) \qquad \left(\gamma I + A_k A_k^\top\right) u_k = p_k - A_k q_0 - \sum_{j=1}^{k-1} A_k A_j^\top u_j.$$

Let $u = (u_1, \ldots, u_K)^\top$. If we decompose

$$\gamma I + AA^\top = \begin{bmatrix} \gamma I + A_1 A_1^\top & \cdots & A_1 A_K^\top \\ \vdots & \ddots & \vdots \\ A_K A_1^\top & \cdots & \gamma I + A_K A_K^\top \end{bmatrix} = D^\gamma + L + L^\top,$$

where $D^\gamma$ and $L$ are the block diagonal and lower triangular parts of $\gamma I + AA^\top$, i.e.,

$$D^\gamma = \begin{bmatrix} \gamma I + A_1 A_1^\top & \cdots & 0 \\ \vdots & \ddots & \vdots \\ 0 & \cdots & \gamma I + A_K A_K^\top \end{bmatrix}, \quad L = \begin{bmatrix} 0 & 0 & \cdots & 0 \\ A_2 A_1^\top & 0 & \cdots & 0 \\ \vdots & \ddots & \ddots & \vdots \\ A_K A_1^\top & \cdots & A_K A_{K-1}^\top & 0 \end{bmatrix},$$

then we can rewrite (3.17) as

$$D^\gamma u = p - A q_0 - L u,$$

which gives

$$u = (D^\gamma + L)^{-1}(p - A q_0).$$

Hence we have

$$q_K = q_0 + \sum_{j=1}^K A_j^\top u_j = q_0 + A^\top u = q_0 + A^\top (D^\gamma + L)^{-1}(p - A q_0) = B^\gamma q_0 + b^\gamma,$$

where

$$B^\gamma = I - A^\top (D^\gamma + L)^{-1} A, \quad b^\gamma = A^\top (D^\gamma + L)^{-1} p.$$

Thus, the regularized block Kaczmarz method (3.16) can be equivalently written as

$$(3.18) \qquad q_\gamma^{l+1} = B^\gamma q_\gamma^l + b^\gamma.$$

Note that the classical Kaczmarz method can be recovered by setting $\gamma = 0$ in (3.18). Consider the iteration

$$(3.19) \qquad v_\gamma^{l+1} = C^\gamma v_\gamma^l + c^\gamma,$$

where

$$C^\gamma = I - (D^\gamma + L)^{-1} AA^\top, \quad c^\gamma = (D^\gamma + L)^{-1} p.$$

It is easy to verify that

$$A^\top C^\gamma = B^\gamma A^\top, \quad A^\top c^\gamma = b^\gamma.$$

Hence, it leads exactly to (3.18) by carrying out (3.19) with $q_\gamma^l = A^\top v_\gamma^l$, which makes it possible to analyze Kaczmarz's method in the framework of classical iterative methods in numerical linear algebra.

LEMMA 3.5. $\mathcal{R}(A^\top)$ is an invariant subspace of $B^\gamma$. The eigenvalues of the restriction of $B^\gamma$ to $\mathcal{R}(A^\top)$ are the eigenvalues of $C^\gamma$ which are not equal to one.

*Proof.* Following from the expression of $B^\gamma$, we can see that $\mathcal{R}(A^\top)$ is an invariant subspace of $B^\gamma$. It is also clear to note from the expression of $C^\gamma$ that $\mathcal{R}((D^\gamma+L)^{-1}A)$ and $\mathcal{N}(A^\top)$ are invariant subspaces of $C^\gamma$. Next we show

$$(3.20) \qquad \mathcal{R}\left((D^\gamma + L)^{-1}A\right) \cap \mathcal{N}\left(A^\top\right) = \{0\}.$$

For if

$$y = (D^\gamma + L)^{-1}Az, \quad A^\top y = 0, \quad z \in \mathbb{R}^n,$$

then

$$\langle (D^\gamma + L)y, y \rangle = \langle Az, y \rangle = \left\langle z, A^\top y \right\rangle = 0,$$

where $\langle \cdot, \cdot \rangle$ is the inner product in the real Euclidean space. Hence

$$\left\langle \left(2D^\gamma + L + L^\top\right) y, y \right\rangle = \langle (D^\gamma + L)y, y \rangle + \left\langle \left(D^\gamma + L^\top\right) y, y \right\rangle = 0.$$

Since $2D^\gamma + L + L^\top$ is positive definite, it follows that $y = 0$.

Now letting $\lambda$ be an eigenvalue of the restriction of $B^\gamma$ to $\mathcal{R}(A^\top)$, we have

$$(1 - \lambda)q = A^\top(D^\gamma + L)^{-1}Aq, \quad 0 \neq q \in \mathcal{R}\left(A^\top\right).$$

Due to (3.20), we must have $\lambda \neq 1$, otherwise $q = 0$. For some $p \neq 0$, taking

$$q = A^\top(D^\gamma + L)^{-1}Ap,$$

we have

$$B^\gamma q - \lambda q = \left(B^\gamma A^\top - \lambda A^\top\right)(D^\gamma + L)^{-1}Ap = 0.$$

It follows from $B^\gamma A^\top = A^\top C^\gamma$ that

$$A^\top(C^\gamma - \lambda I)(D^\gamma + L)^{-1}Ap = 0.$$

Since $\mathcal{R}((D^\gamma + L)^{-1}A)$ is an invariant subspace of $C^\gamma$ satisfying (3.20), it yields that

$$(C^\gamma - \lambda I)(D^\gamma + L)^{-1}Ap = 0,$$

which gives that $\lambda$ is an eigenvalue of $C^\gamma$.

Conversely, if $C^\gamma y = \lambda y$ with $\lambda \neq 1, y \neq 0$, then

$$(1 - \lambda)y = (D^\gamma + L)^{-1}AA^\top y.$$

Hence $y \in \mathcal{R}((D^\gamma + L)^{-1}A)$ and, because of (3.20), $p = A^\top y \neq 0$. It follows that

$$B^\gamma p - \lambda p = B^\gamma A^\top y - \lambda A^\top y = A^\top C^\gamma y - \lambda A^\top y = A^\top(C^\gamma y - \lambda y) = 0,$$

which shows that $\lambda$ is an eigenvalue of the restriction of $B^\gamma$ to $\mathcal{R}(A^\top)$. $\qquad\square$

The spectral radius of a matrix is the maximum of the absolute values of the eigenvalues of the matrix.

LEMMA 3.6. *The spectral radius for the restriction of $B^\gamma$ to $\mathcal{R}(A^\top)$ is less than one.*

*Proof.* According to Lemma 3.5, it suffices to show that the eigenvalues of $C^\gamma$, which are not equal to one, are less than one in the absolute value. Let $C^\gamma y = \lambda y$ with $\lambda \neq 1, y \neq 0$. Then

$$(3.21) \qquad \left(\gamma I - L^\top\right) y = \lambda (D^\gamma + L) y.$$

Let $D^\gamma = \gamma I + D$, where

$$D = \begin{bmatrix} A_1 A_1^\top & \cdots & 0 \\ \vdots & \ddots & \vdots \\ 0 & \cdots & A_K A_K^\top \end{bmatrix}.$$

It can be easily verify that $AA^\top = D + L + L^\top$.

We normalize $y$ such that $\langle Dy, y \rangle = 1$ and put $\langle Ly, y \rangle = \alpha$. Taking the inner product of (3.21) with $y$ yields

$$\gamma \langle y, y \rangle - \alpha = \lambda (\gamma \langle y, y \rangle + 1 + \alpha).$$

Hence

$$|\lambda| = \left| \frac{\gamma \langle y, y \rangle - \alpha}{\gamma \langle y, y \rangle + 1 + \alpha} \right|.$$

Since $A^\top A = D + L + L^\top$ is positive semidefinite, we have $1 + 2\alpha \geq 0$, which gives $\alpha \geq -1/2$. We can exclude $\alpha = -1/2$ since in this case $\lambda = 1$. For $\alpha > -1/2$, we have $|\gamma \langle y, y \rangle - \alpha| < |\gamma \langle y, y \rangle + 1 + \alpha|$, which implies that $|\lambda| < 1$. $\qquad\square$

Now we come to the main result of the convergence for the regularized block Kaczmarz method.

THEOREM 3.7. *Assume that the system* (3.13) *is consistent with the minimal norm solution* $q^\dagger$ *and the initial guess* $q^0_\gamma \in \mathcal{R}(A^\top)$, *e.g.,* $q^0_\gamma = 0$. *Then* $q^l_\gamma$ *converges, as* $l \to \infty$, *to* $q^\dagger_\gamma$, *which converges to* $q^\dagger$ *as* $\gamma \to 0$.

*Proof.* Since $q^0_\gamma \in \mathcal{R}(A^\top)$ and $b^\gamma = A^\top (D^\gamma + L)^{-1} p \in \mathcal{R}(A^\top)$, the iteration (3.18) takes place in $\mathcal{R}(A^\top)$, where $B^\gamma$ is a contraction by Lemma 3.6. Hence the sequence $\{q^l_\gamma\}$ converges, as $l \to \infty$, to $q^\dagger_\gamma \in \mathcal{R}(A^\top)$, which satisfies

$$q^\dagger_\gamma = B^\gamma q^\dagger_\gamma + b^\gamma.$$

The solution $q^\dagger$ of the classical Kaczmarz method satisfies

$$q^\dagger = B q^\dagger + b,$$

where

$$B = I - A^\top (D + L)^{-1} A, \quad b = A^\top (D + L)^{-1} p.$$

It follows from $\|B^\gamma - B\| \to 0$ and $\|b^\gamma - b\| \to 0$ as $\gamma \to 0$ that $\|q^\gamma - q\| \to 0$ as $\gamma \to 0$, which completes the proof. $\qquad\square$

Although there are two loops in (3.16), the matrices $\gamma I + A_k A_k^\top$ lead to a small scale linear system of equations with the size equal to the number of measurements. Moreover, they essentially need to be solved only $K$ times by a direct solver such as the LU decomposition since $A_k$ keep the same during the outer loop. In practice, we take a finite number of iterations for the outer loop, i.e., $l = 0, 1, \ldots, L$, where $L > 0$ is a prescribed integer.

**4. Numerical experiments.** We present a numerical example to demonstrate the effectiveness of the proposed method. The scattering data is obtained by the numerical solution of the stochastic Navier equation in order to avoid the so-called inverse crime. Although the stochastic Navier equation may be efficiently solved by using the Wiener chaos expansions to obtain statistical moments such as the mean and variance [6], we choose the Monte Carlo method to simulate the actual process of measuring data. In each realization, the stochastic Navier equation is solved by using the finite element method with the perfectly matched layer (PML) technique. The scattering data is then collected on the boundary $\partial B_R$. After all the realizations are done, an average is taken to approximate the mean or the variance.

Let

$$g_1(x_1, x_2) = 0.3(1 - x_1)^2 e^{-x_1^2 - (x_2+1)^2} - \left(0.2x_1 - x_1^3 - x_2^5\right) e^{-x_1^2 - x_2^2} - 0.03 e^{-(x_1+1)^2 - x_2^2}$$

and

$$g_2(x_1, x_2) = 5x_1^2 x_2 e^{-x_1^2 - x_2^2}.$$

We reconstruct the mean $\boldsymbol{g}(x_1, x_2) = (g_1(3x_1, 3x_2), g_2(3x_1, 3x_2))^\top$ inside the domain $D = [-1, 1] \times [-1, 1]$. Let

$$h_1(x_1, x_2) = 0.6 e^{-8(r^3 - 0.75r^2)}$$

and

$$h_2(x_1, x_2) = e^{-r^2}, \quad r = \left(x_1^2 + x_2^2\right)^{1/2}.$$

We reconstruct the variance $\boldsymbol{h}^2$ given by

$$\boldsymbol{h}^2(x_1, x_2) = \begin{bmatrix} h_1^2(x_1, x_2) & 0 \\ 0 & h_2^2(3x_1, 3x_2) \end{bmatrix}$$

inside the domain $D = [-1, 1] \times [-1, 1]$. See Figure 3 for the surface plot of the exact $g_1, g_2$ (top) and $h_1^2, h_2^2$ (below). The Lamé constants are $\mu = 1.0$ and $\lambda = 2.0$. The computational domain is set to be $[-3, 3] \times [-3, 3]$ with the PML thickness 0.5. After the direct problem is solved and the value of $\boldsymbol{u}$ is obtained at the grid points, the linear interpolation is used to generate the synthetic data at 20 uniformly distributed points on the circle with radius 2, i.e., $x_1 = 2\cos\theta_i, x_2 = 2\sin\theta_i, \theta_i = i\pi/10, i = 0, 1, \ldots, 19$. Sixteen equally spaced frequencies from $0.5\pi$ to $7.5\pi$ are used in the reconstruction of $g_1, g_2$, while twenty equally spaced frequencies from $0.5\pi$ to $2.5\pi$ are used in the reconstruction of $h_1^2, h_2^2$. At each frequency, the composite trapezoidal rule is used to discretize the integral equations (3.3)–(3.6) and (3.11)–(3.12) to obtain the matrix equation (3.13). In the regularized Kaczmarz method, the regularization parameter is $\gamma = 1.0 \times 10^{-7}$ and the total number of the outer loop is $L = 5$. Figure 4 shows the reconstructed mean $g_1, g_2$ (top) and the reconstructed variance $h_1^2, h_2^2$ (below) corresponding to the number of realization $10^4$. It can be seen from the results that the proposed method can effectively reconstruct both the mean and the variance of the random source by using the multiple frequency data.

**5. Conclusion.** We have studied the direct and inverse random source scattering problems for the stochastic Navier equation where the source is driven by an additive white noise. Under a suitable regularity assumption of the source functions $\boldsymbol{g}$ and $\boldsymbol{h}$, the direct scattering problem is shown constructively to have a unique mild solution which was given explicitly as an integral equation. Based on the explicit
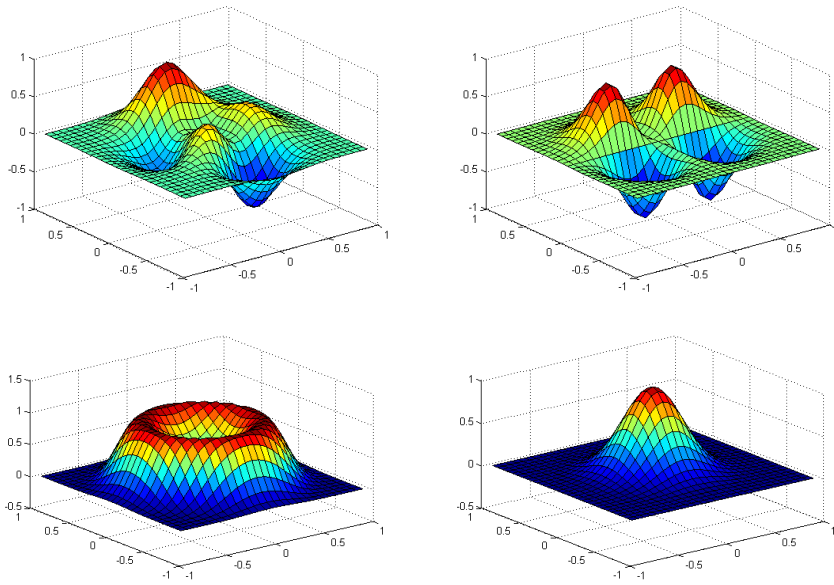
FIG. 3. *The exact source: (top) surface plot of the exact mean $g_1$ and $g_2$; (below) surface plot of the exact variance $h_1^2$ and $h_2^2$.*
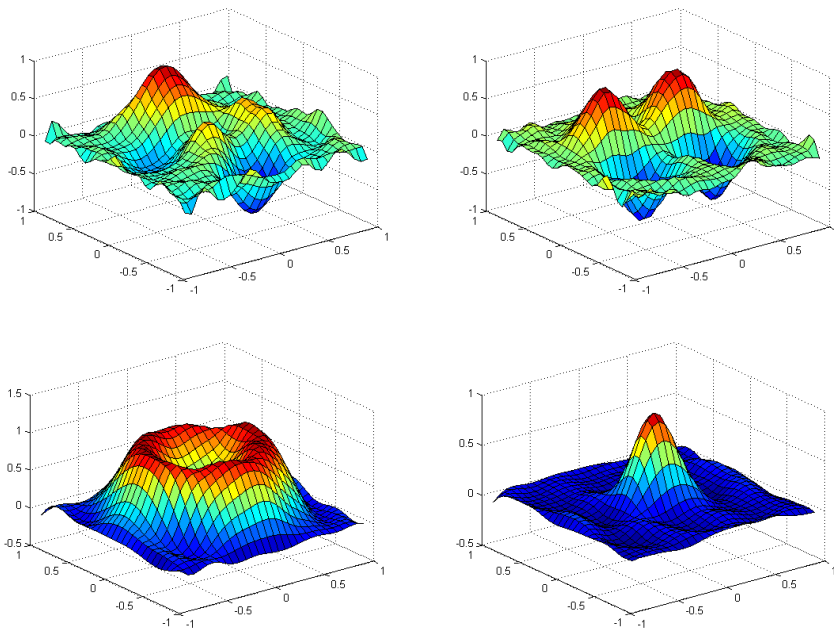


FIG. 4. *The reconstructed source: (top) surface plot of the reconstructed mean $g_1, g_2$; (below) surface plot of the reconstructed variance $h_1^2, h_2^2$.*

solution, Fredholm integral equations are deduced for the inverse scattering problem to reconstruct the mean and the variance of the random source. We have presented the regularized Kaczmarz method to solve the ill-posed integral equations by using multiple frequency data. The convergence of the method is proved under the assumption that the resulting linear system is consistent. A representative numerical example is presented to demonstrate the validity and effectiveness of the proposed method. We are currently investigating the inverse random source scattering problem in an inhomogeneous elastic medium where the explicit Green tensor function is no longer available. Although this paper concerns the inverse random source scattering problem for the Navier equation, we believe that the proposed framework and methodology can be directly applied to solve many other inverse random source problems and even more general stochastic inverse problems. For instance, it is interesting to study inverse random source problems for the stochastic Poisson, heat, or electromagnetic wave equation. Obviously, it is more challenging to consider the inverse random medium scattering problem where the medium should be modeled as a random function. We hope to be able to report the progress on these problems in the future.

**Appendix A. Brownian sheet.** Let us first briefly introduce the one-dimensional Brownian sheet on $(\mathbb{R}_+^d, \mathcal{B}(\mathbb{R}_+^d), \mu)$, where $d \in \mathbb{N}, \mathbb{R}_+^d = \{x = (x_1, \ldots, x_d)^\top \in \mathbb{R}^d : x_j \geq 0, j = 1, \ldots, d\}$, $\mathcal{B}(\mathbb{R}_+^d)$ is the Borel $\sigma$-algebra of $\mathbb{R}_+^d$, and $\mu$ is the Lebesgue measure. More details can be found in [35]. Let $(0, x] = (0, x_1] \times \cdots \times (0, x_d]$ for $x \in \mathbb{R}_+^d$.

DEFINITION A.1. *The one-dimensional d-parameter Brownian sheet defined on a probability space $(\Sigma, \mathcal{F}, P)$ is the process $\{W_x : x \in \mathbb{R}_+^d\}$ defined by $W_x = W\{(0, x]\}$, where $W$ is a random set function such that*
  1. *$\forall A \in \mathcal{B}(\mathbb{R}_+^d), W(A): (\Sigma, \mathcal{F}, P) \to (\mathbb{R}, \mathcal{B}(\mathbb{R}), \mu)$ is a Gaussian random variable with mean 0 and variance $\mu(A)$, i.e., $W(A) \sim \mathcal{N}(0, \mu(A))$;*
  2. *$\forall A, B \in \mathcal{B}(\mathbb{R}_+^d)$, if $A \cap B = \emptyset$, then $W(A)$ and $W(B)$ are independent and $W(A \cup B) = W(A) + W(B)$.*

It can be verified from Definition A.1 that

$$\mathbf{E}(W(A)W(B)) = \mu(A \cap B) \quad \forall A, B \in \mathcal{B}\left(\mathbb{R}_+^d\right),$$

which gives the covariance function of the Brownian sheet:

$$\mathbf{E}(W_x W_y) = x \wedge y := (x_1 \wedge y_1) \cdots (x_d \wedge y_d)$$

for any $x = (x_1, \ldots, x_d)^\top \in \mathbb{R}_+^d$ and $y = (y_1, \ldots, y_d)^\top \in \mathbb{R}_+^d$, where $x_j \wedge y_j = \min\{x_j, y_j\}$.

The Brownian sheet can be generalized to the space $\mathbb{R}^d$ by introducing $2^d$ independent Brownian sheets defined on $\mathbb{R}_+^d$. Define a multi-index $t = (t_1, \ldots, t_d)^\top$ with $t_j = \{1, -1\}$ for $j = 1, \ldots, d$. Introduce $2^d$ independent Brownian sheets $\{W^t\}$ defined on $\mathbb{R}_+^d$. For any $x = (x_1, \ldots, x_d)^\top \in \mathbb{R}^d$, define the Brownian sheet

$$W_x := W_{\check{x}}^{t(x)},$$

where $\check{x} = (|x_1|, \ldots, |x_d|)^\top$ and $t(x) = (\text{sgn}(x_1), \ldots, \text{sgn}(x_d))^\top$. The sign function $\text{sgn}(x_j) = 1$ if $x_j \geq 0$, otherwise $\text{sgn}(x_j) = -1$.

The white noise can be thought of as the derivative of the Brownian sheet. In fact, the Brownian sheet $W_x$ is nowhere-differentiable in the ordinary sense, but its

derivatives will exist in the sense of Schwartz distributions. Define

$$\dot{W}_x = \frac{\partial^d W_x}{\partial x_1 \cdots \partial x_d}.$$

If $\phi(x)$ is a deterministic square-integrable complex-valued test function with a compact support in $\mathbb{R}^d$, then $\dot{W}_x$ is the distribution

$$\dot{W}_x(\phi) = (-1)^d \int_{\mathbb{R}^d} W_x \frac{\partial^d \phi(x)}{\partial x_1 \cdots \partial x_d} \mathrm{d}x.$$

We may define the stochastic integral

(A.1) $$\int_{\mathbb{R}^d} \phi(x)\mathrm{d}W_x = (-1)^d \int_{\mathbb{R}^d} W_x \frac{\partial^d \phi(x)}{\partial x_1 \cdots \partial x_d} \mathrm{d}x,$$

which satisfies the following properties (cf. [7, Proposition A.2]).

LEMMA A.2. *Let $\phi(x)$ be a test function with a compact support in $\mathbb{R}^d$. We have*

$$\mathbf{E}\left(\int_{\mathbb{R}^d} \phi(x)\mathrm{d}W_x\right) = 0, \quad \mathbf{E}\left(\left|\int_{\mathbb{R}^d} \phi(x)\mathrm{d}W_x\right|^2\right) = \int_{\mathbb{R}^d} |\phi(x)|^2 \mathrm{d}x.$$

The stochastic integral (A.1) can be extended to define the multidimensional stochastic integrals. Let $W(x) = (W_1(x), \ldots, W_n(x))^\top$ be an $n$-dimensional Brownian sheet, where $W_i(x)$ and $W_j(x)$ are two one-dimensional independent Brownian sheets for $i \neq j$. Let $\phi$ be a deterministic square-integrable complex-valued $m \times n$ matrix-valued test function with each component compactly supported in $\mathbb{R}^d$, i.e.,

$$\phi(x) = \begin{bmatrix} \phi_{11}(x) & \cdots & \phi_{1n}(x) \\ \vdots & & \vdots \\ \phi_{m1}(x) & \cdots & \phi_{mn}(x) \end{bmatrix}.$$

Using the matrix notation, we may define the multidimensional stochastic integral

(A.2) $$\int_{\mathbb{R}^d} \phi(x)\mathrm{d}W(x) = \int_{\mathbb{R}^d} \begin{bmatrix} \phi_{11}(x) & \cdots & \phi_{1n}(x) \\ \vdots & & \vdots \\ \phi_{m1}(x) & \cdots & \phi_{mn}(x) \end{bmatrix} \begin{bmatrix} \mathrm{d}W_1(x) \\ \vdots \\ \mathrm{d}W_n(x) \end{bmatrix},$$

which is an $m \times 1$ matrix and its $j$th component is the sum of one-dimensional stochastic integrals

$$\sum_{k=1}^n \int_{\mathbb{R}^d} \phi_{jk}(x)\mathrm{d}W_k(x).$$

We have the similar properties for the multidimensional stochastic integral.

PROPOSITION A.3. *Let $W(x) = (W_1(x), \ldots, W_n(x))^\top$ be an $n$-dimensional Brownian sheet and $\phi(x) = (\phi_{ij}(x))_{m \times n}$ be an $m \times n$ matrix-valued function with each component $\phi_{ij}(x)$ compactly supported in $\mathbb{R}^d$. We have*

$$\mathbf{E}\left(\int_{\mathbb{R}^d} \phi(x)\mathrm{d}W_x\right) = 0, \quad \mathbf{E}\left(\left|\int_{\mathbb{R}^d} \phi(x)\mathrm{d}W_x\right|^2\right) = \int_{\mathbb{R}^d} \|\phi(x)\|^2 \mathrm{d}x,$$

*where $\|\cdot\|$ is the Frobenius norm.*

*Proof.* It follows from (A.2) and Lemma A.2 that

$$\mathbf{E}\left(\int_{\mathbb{R}^d}\phi(x)\mathrm{d}W_x\right) = \begin{bmatrix} \sum_{k=1}^n \mathbf{E}\left(\int_{\mathbb{R}^d}\phi_{jk}(x)\mathrm{d}W_k(x)\right) \\ \vdots \\ \sum_{k=1}^n \mathbf{E}\left(\int_{\mathbb{R}^d}\phi_{jk}(x)\mathrm{d}W_k(x)\right) \end{bmatrix} = 0.$$

Using (A.2) and Lemma A.2 again, we have

$$\mathbf{E}\left(\left|\int_{\mathbb{R}^d}\phi(x)\mathrm{d}W_x\right|^2\right) = \sum_{j=1}^m \mathbf{E}\left(\left|\sum_{k=1}^n \int_{\mathbb{R}^d}\phi_{jk}(x)\mathrm{d}W_k(x)\right|^2\right)$$

$$= \sum_{j=1}^m \sum_{k=1}^n \int_{\mathbb{R}^d}|\phi_{jk}(x)|^2\mathrm{d}x$$

$$= \int_{\mathbb{R}^d}\|\phi(x)\|^2\mathrm{d}x,$$

which completes the proof. $\qquad\square$

**Appendix B. Entries of Green's tensor.** The matrices $\mathrm{Re}\,\mathbb{G}$ and $\mathrm{Im}\,\mathbb{G}$ are real symmetric. Denote

$$\kappa_{\mathrm{p},k} = \frac{\omega_k}{\sqrt{\lambda+2\mu}}, \quad \kappa_{\mathrm{s},k} = \frac{\omega_k}{\sqrt{\mu}}.$$

A simple calculation yields that

$$G_{\mathrm{Re}}^{[11]}(x,y,\omega_k) = -\frac{1}{4\mu}Y_0(\kappa_{\mathrm{s},k}|x-y|)$$

$$+ \frac{1}{4\omega_k^2|x-y|}\Big(\kappa_{\mathrm{s},k}Y_1(\kappa_{\mathrm{s},k}|x-y|) - \kappa_{\mathrm{p},k}Y_1(\kappa_{\mathrm{p},k}|x-y|)\Big)$$

$$- \frac{(x_1-y_1)^2}{4\omega_k^2|x-y|^2}\bigg[\frac{2\kappa_{\mathrm{s},k}}{|x-y|}Y_1(\kappa_{\mathrm{s},k}|x-y|) - \kappa_{\mathrm{s},k}^2 Y_0(\kappa_{\mathrm{s},k}|x-y|)$$

$$- \frac{2\kappa_{\mathrm{p},k}}{|x-y|}Y_1(\kappa_{\mathrm{p},k}|x-y|) + \kappa_{\mathrm{p},k}^2 Y_0(\kappa_{\mathrm{p},k}|x-y|)\bigg],$$

$$G_{\mathrm{Re}}^{[12]}(x,y,\omega_k) = -\frac{(x_1-y_1)(x_2-y_2)}{4\omega_k^2|x-y|^2}\bigg[\frac{2\kappa_{\mathrm{s},k}}{|x-y|}Y_1(\kappa_{\mathrm{s},k}|x-y|) - \kappa_{\mathrm{s},k}^2 Y_0(\kappa_{\mathrm{s},k}|x-y|)$$

$$- \frac{2\kappa_{\mathrm{p},k}}{|x-y|}Y_1(\kappa_{\mathrm{p},k}|x-y|) + \kappa_{\mathrm{p},k}^2 Y_0(\kappa_{\mathrm{p},k}|x-y|)\bigg],$$

$$G_{\mathrm{Re}}^{[22]}(x,y,\omega_k) = -\frac{1}{4\mu}Y_0(\kappa_{\mathrm{s},k}|x-y|)$$

$$+ \frac{1}{4\omega_k^2|x-y|}\Big(\kappa_{\mathrm{s},k}Y_1(\kappa_{\mathrm{s},k}|x-y|) - \kappa_{\mathrm{p},k}Y_1(\kappa_{\mathrm{p},k}|x-y|)\Big)$$

$$- \frac{(x_2-y_2)^2}{4\omega_k^2|x-y|^2}\bigg[\frac{2\kappa_{\mathrm{s},k}}{|x-y|}Y_1(\kappa_{\mathrm{s},k}|x-y|) - \kappa_{\mathrm{s},k}^2 Y_0(\kappa_{\mathrm{s},k}|x-y|)$$

$$- \frac{2\kappa_{\mathrm{p},k}}{|x-y|}Y_1(\kappa_{\mathrm{p},k}|x-y|) + \kappa_{\mathrm{p},k}^2 Y_0(\kappa_{\mathrm{p},k}|x-y|)\bigg]$$

and

$$G_{\mathrm{Im}}^{[11]}(x,y,\omega_k) = \frac{1}{4\mu}J_0(\kappa_{\mathrm{s},k}|x-y|)$$

$$-\frac{1}{4\omega_k^2|x-y|}\Big(\kappa_{\mathrm{s},k}J_1(\kappa_{\mathrm{s},k}|x-y|) - \kappa_{\mathrm{p},k}J_1(\kappa_{\mathrm{p},k}|x-y|)\Big)$$

$$+\frac{(x_1-y_1)^2}{4\omega_k^2|x-y|^2}\Bigg[\frac{2\kappa_{\mathrm{s},k}}{|x-y|}J_1(\kappa_{\mathrm{s},k}|x-y|) - \kappa_{\mathrm{s},k}^2 J_0(\kappa_{\mathrm{s},k}|x-y|)$$

$$-\frac{2\kappa_{\mathrm{p},k}}{|x-y|}J_1(\kappa_{\mathrm{p},k}|x-y|) + \kappa_{\mathrm{p},k}^2 J_0(\kappa_{\mathrm{p},k}|x-y|)\Bigg],$$

$$G_{\mathrm{Im}}^{[12]}(x,y,\omega_k) = \frac{(x_1-y_1)(x_2-y_2)}{4\omega_k^2|x-y|^2}\Bigg[\frac{2\kappa_{\mathrm{s},k}}{|x-y|}J_1(\kappa_{\mathrm{s},k}|x-y|) - \kappa_{\mathrm{s},k}^2 J_0(\kappa_{\mathrm{s},k}|x-y|)$$

$$-\frac{2\kappa_{\mathrm{p},k}}{|x-y|}J_1(\kappa_{\mathrm{p},k}|x-y|) + \kappa_{\mathrm{p},k}^2 J_0(\kappa_{\mathrm{p},k}|x-y|)\Bigg],$$

$$G_{\mathrm{Im}}^{[22]}(x,y,\omega_k) = \frac{1}{4\mu}J_0(\kappa_{\mathrm{s},k}|x-y|)$$

$$-\frac{1}{4\omega_k^2|x-y|}\Big(\kappa_{\mathrm{s},k}J_1(\kappa_{\mathrm{s},k}|x-y|) - \kappa_{\mathrm{p},k}J_1(\kappa_{\mathrm{p},k}|x-y|)\Big)$$

$$+\frac{(x_2-y_2)^2}{4\omega_k^2|x-y|^2}\Bigg[\frac{2\kappa_{\mathrm{s},k}}{|x-y|}J_1(\kappa_{\mathrm{s},k}|x-y|) - \kappa_{\mathrm{s},k}^2 J_0(\kappa_{\mathrm{s},k}|x-y|)$$

$$-\frac{2\kappa_{\mathrm{p},k}}{|x-y|}J_1(\kappa_{\mathrm{p},k}|x-y|) + \kappa_{\mathrm{p},k}^2 J_0(\kappa_{\mathrm{p},k}|x-y|)\Bigg].$$

Here $J_0$, $Y_0$ and $J_1$, $Y_1$ are the Bessel function of the first and second kind with order zero and order 1, respectively.

**Appendix C. Minimal norm solution.** Consider an underdetermined linear system

$$(C.1) \qquad\qquad\qquad Aq = p,$$

where $A : \mathbb{R}^n \to \mathbb{R}^m$ is an $m \times n$ matrix, $m < n$, with linearly independent rows, $q \in \mathbb{R}^n$, and $p \in \mathbb{R}^m$. Let $\|\cdot\|$ is the Euclidean vector norm. The system (C.1) has infinitely many solutions, among which we are seeking the solution $q^\dagger$ such that $\|q^\dagger\|$ is minimized. The solution $q^\dagger$ is called the minimal norm solution of the system (C.1).

Let $\mathcal{N}(A) = \{q \in \mathbb{R}^n : Aq = 0\}$ be the null space of $A$. Let $q_0$ be a particular solution of $Aq = p$. Then any solution of (C.1) has the form

$$q = q_0 - z, \quad z \in \mathcal{N}(A).$$

The problem of finding the minimal norm solution is transformed to find a vector $z_0 \in \mathcal{N}(A)$ such that $\|q_0 - z_0\|$ is minimized. We can conclude that

$$q^\dagger = q_0 - z_0 \in \mathcal{N}(A)^\perp = \mathcal{R}\left(A^\top\right),$$

where $\mathcal{R}(A^\top)$ is called the range of $A^\top$. Hence we have $q^\dagger = A^\top p_0$ for some vector $p_0 \in \mathbb{R}^m$. It follows that

$$AA^\top p_0 = p.$$

Since the rows of $A$ are linearly independent, $AA^\top$ is nonsingular $m \times m$ matrix. Therefore, we obtain $p_0 = (AA^\top)^{-1}p$ and the minimal norm solution

$$q^\dagger = A^\dagger p,$$

where $A^\dagger = A^\top(AA^\top)^{-1}$ is the pseudoinverse of $A$.

GANG BAO, CHUCHU CHEN, AND PEIJUN LI

## REFERENCES

[1] R. Albanese and P. Monk, *The inverse source problem for Maxwell's equations*, Inverse Problems, 22 (2006), pp. 1023–1035.

[2] H. Ammari, G. Bao, and J. Fleming, *An inverse source problem for Maxwell's equations in magnetoencephalography*, SIAM J. Appl. Math., 62 (2002), pp. 1369–1382.

[3] H. Ammari, E. Bretin, J. Garnier, H. Kang, H. Lee, and A. Wahab, *Mathematical Methods in Elasticity Imaging*, Princeton University Press, Princeton, NJ, 2015.

[4] H. Ammari, E. Bretin, J. Garnier, and A. Wahab, *Noise source localization in an attenuating medium*, SIAM J. Appl. Math., 72 (2012), pp. 317–336.

[5] A. Badia and T. Nara, *An inverse source problem for Helmholtz's equation from the Cauchy data with a single wave number*, Inverse Problems, 27 (2011), p. 105001.

[6] M. Badieirostami, A. Adibi, H.-M. Zhou, and S.-N. Chow, *Wiener chaos expansion and simulation of electromagnetic wave propagation excited by a spatially incoherent source*, Multiscale Model. Simul., 8 (2010), pp. 591–604.

[7] G. Bao, C. Chen, and P. Li, *Inverse random source scattering problems in several dimensions*, SIAM/ASA J. Uncertain. Quantif., 4 (2016), pp. 1263–1287.

[8] G. Bao, S.-N. Chow, P. Li, and H.-M. Zhou, *An inverse random source problem for the Helmholtz equation*, Math. Comp., 83 (2014), pp. 215–233.

[9] G. Bao, P. Li, J. Lin, and F. Triki, *Inverse scattering problems with multi-frequencies*, Inverse Problems, 31 (2015), 093001.

[10] G. Bao, J. Lin, and F. Triki, *A multi-frequency inverse source problem*, J. Differential Equatons, 249 (2010), pp. 3443–3465.

[11] G. Bao, S. Lu, W. Rundell, and B. Xu, *A recursive algorithm for multifrequency acoustic inverse source problems*, SIAM J. Numer. Anal., 53 (2015), pp. 1608–1628.

[12] G. Bao and X. Xu, *An inverse random source problem in quantifying the elastic modulus of nano-materials*, Inverse Problems, 29 (2013), p. 015006.

[13] M. Bonnet and A. Constantinescu, *Inverse problems in elasticity*, Inverse Problems, 21 (2005), pp. 1–50.

[14] Y.-Z. Cao, R. Zhang, and K. Zhang, *Finite element method and discontinuous Galerkin method for stochastic Helmholtz equation in two- and three-dimensions*, J. Comput. Math., 26 (2008), pp. 701–715.

[15] D. Colton and R. Kress, *Inverse Acoustic and Electromagnetic Scattering Theory*, Springer, Berlin, 1998.

[16] A. Devaney, *The inverse problem for random sources*, J. Math. Phys., 20 (1979), pp. 1687–1691.

[17] A. Devaney, E. Marengo, and M. Li, *Inverse source problem in nonhomogeneous background media*, SIAM J. Appl. Math., 67 (2007), pp. 1353–1378.

[18] A. Devaney and G. Sherman, *Nonuniqueness in inverse source and scattering problems*, IEEE Trans. Antennas and Propagation, 30 (1982), pp. 1034–1037.

[19] M. Eller and N. Valdivia, *Acoustic source identification using multiple frequency information*, Inverse Problems, 25 (2009), 115005.

[20] L. Evans, *An Introduction to Stochastic Differential Equations*, AMS, Providence, RI, 2013.

[21] A. Fokas, Y. Kurylev, and V. Marinakis, *The unique determination of neuronal currents in the brain via magnetoencephalogrphy*, Inverse Problems, 20 (2004), pp. 1067–1082.

[22] A. Friedman, *Stochastic Differential Equations and Applications*, Academic Press, New York, 2006.

[23] K.-H. Hauer, L. Kühn, and R. Potthast, *On uniqueness and non-uniqueness for current reconstruction from magnetic fields*, Inverse Problems, 21 (2005), pp. 955–967.

[24] M. Hairer, *Introduction to Stochastic PDEs*, Lecture notes, 2009.

[25] V. Isakov, *Inverse Source Problems*, AMS, Providence, RI, 1989.

[26] J. Kaipio and E. Somersalo, *Statistical and Computational Inverse Problems*, Springer, Berlin, 2005.

[27] R. Kress, *Inverse elastic scattering from a crack*, Inverse Problems, 12 (1996), pp. 667–684.

[28] L. D. Landau and E. M. Lifshitz, *Theory of Elasticity*, Pergamon, Oxford, UK, 1986.

[29] P. Li, *An inverse random source scattering problem in inhomogeneous media*, Inverse Problems, 27 (2011), 035004.

[30]  P. LI, Y. WANG, AND Y. ZHAO, *Inverse elastic surface scattering with near-field data*, Inverse Problems, 31 (2015), 035009.

[31]  P. LI AND G. YUAN, *Stability on the inverse random source scattering problem for the one-dimensional Helmholtz equation*, J. Math. Anal. Appl., 450 (2017), pp. 872–887.

[32]  P. LI AND G. YUAN, *Increasing stability for the inverse source scattering problem with multi-frequencies*, Inverse Probl. Imaging, 11 (2017), pp. 745–759.

[33]  E. MARENGO AND A. DEVANEY, *The inverse source problem of electromagnetics: Linear inversion formulation and minimum energy solution*, IEEE Trans. Antennas and Propagation, 47 (1999), pp. 410–412.

[34]  F. NATTERER, *The Mathematics of Computerized Tomography*, Teubner, Stuttgart, 1986.

[35]  J. WALSH, *An Introduction to Stochastic Partial Differential Equations*, Springer, Berlin, 1986.

[36]  D. ZHANG AND Y. GUO, *Fourier method for solving the multi-frequency inverse acoustic source problem for the Helmholtz equation*, Inverse Problems, 31 (2015), 035007.